International Workshop

Droughts over Pakistan in the Changing Climate

(21-22 February 2024)

Climate-Induced Drought Variability in Pakistan and Large-Scale Circulation Patterns

Dr. Muhammad Latif

Asst. Prof.

Department of Meteorology, COMSATS University Islamabad, Pakistan

Email: muhammad_latif@comsats.edu.pk

Website URL: http://ww2.comsats.edu.pk/faculty/FacultyDetails.aspx?Uid=646

Google Scholar: https://scholar.google.com/citations?user=5Xh-27wAAAAJ&hl=en

http://ww2.comsats.edu.pk/Meteorology/

Presentation Outline

Background

- Understanding Drought
- Natural Climatic Hazards in Pakistan
- Climate Change Impacts in Pakistan

Key Findings

- Historical Drought Patterns
- Satellite-Based Drought Monitoring
- Future Projections: Climate Models

- Conclusions






What is **Drought**?

A prolonged period of abnormally low precipitation results in a water shortage that can lead to adverse impacts on agriculture, water supply, ecosystems, and human activities.

Meteorological

Hydrological

Agricultural

Socioeconomic

The frequency and intensity of all four types of drought are increasing in most parts of the country due to climate change.

Climate Change: GCRI, GHGs, and Paris Agreement

CRI	Country
1	Puerto Rico
2	Myanmar
3	Haiti
4	Philippines
5	Mozambique
6	The Bahamas
7	Bangladesh
8	Pakistan
9	Thailand
10	Nepal

Source: German Watch Report

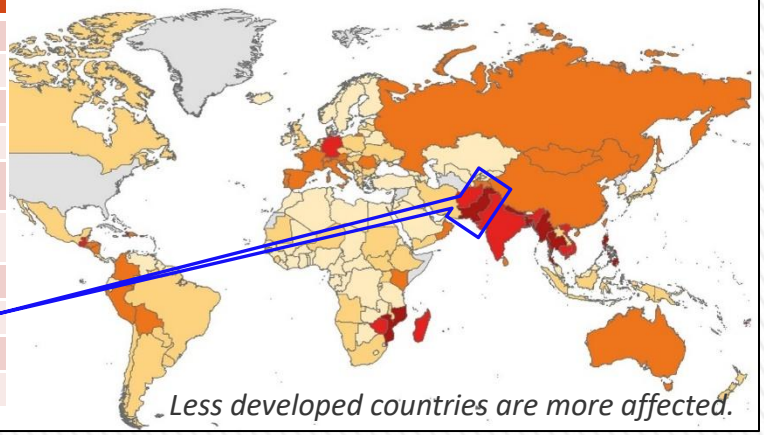

World Resources Institute's Climate Analysis Indicators Tool, 2022

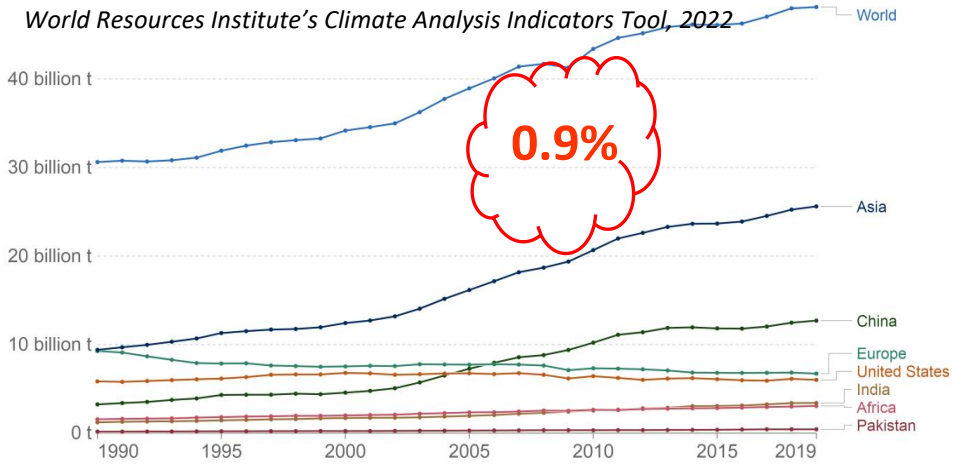

Pakistan contributes only about 0.9% to global GHG emissions, yet it is the most vulnerable country to the negative impacts of climate change.

Global Climate Risk Index:

Pakistan has been ranked as the 8th most vulnerable country due to climate change, and it is expected to be one of the top three countries in the coming report.

Paris Agreement (PA) targets of **1.5°C and 2.0 °C** are reaching Pakistan **ten years** earlier than the global average temperatures.

Kiani et al. (2021)

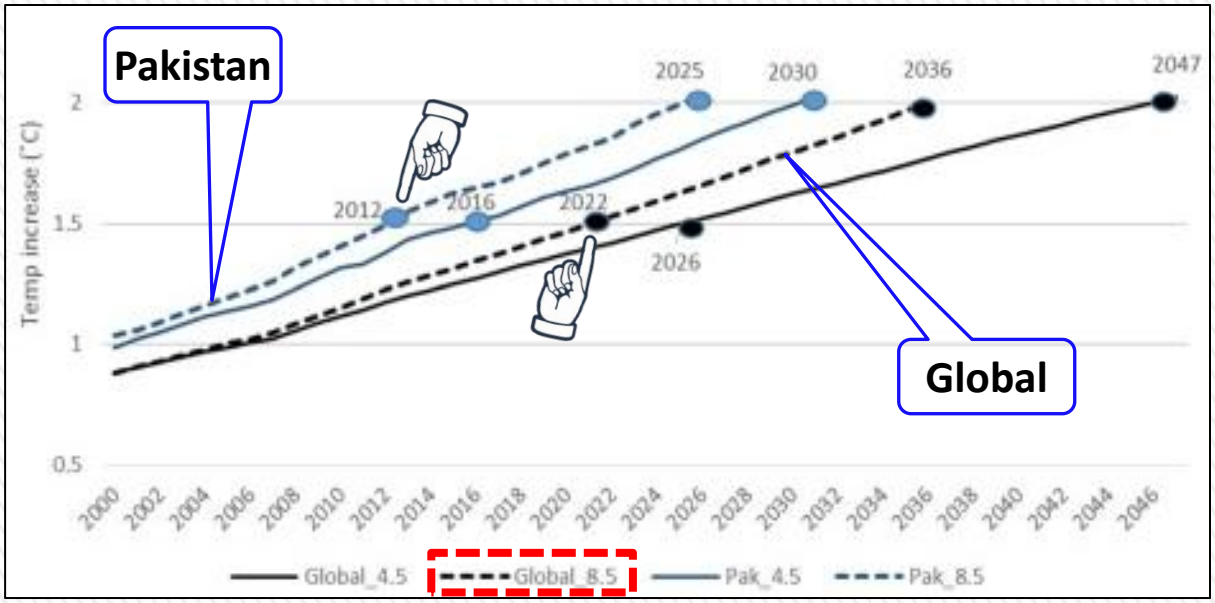

Natural Climatic Hazards in Pakistan

Average Annual Natural Hazard Occurrence for 1980–2020

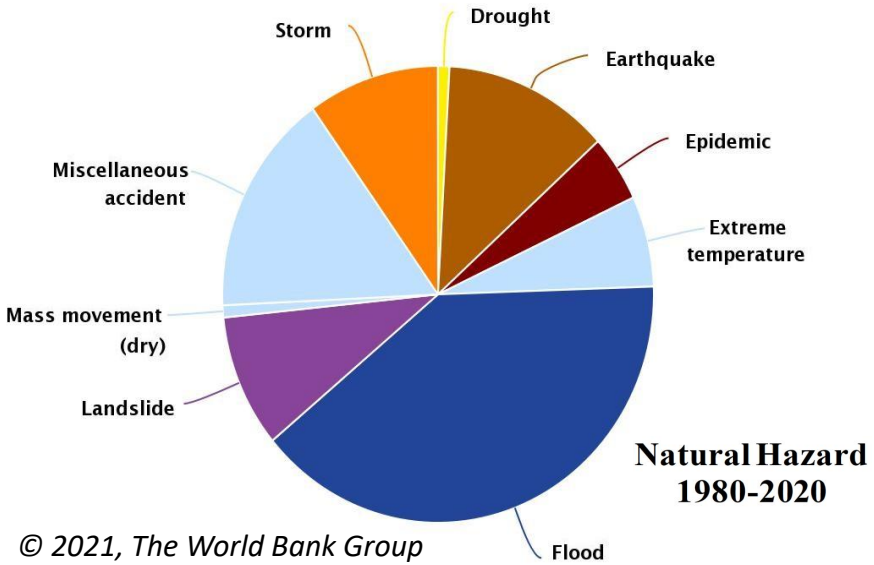

Key Natural Hazard Statistics for 1980–2020

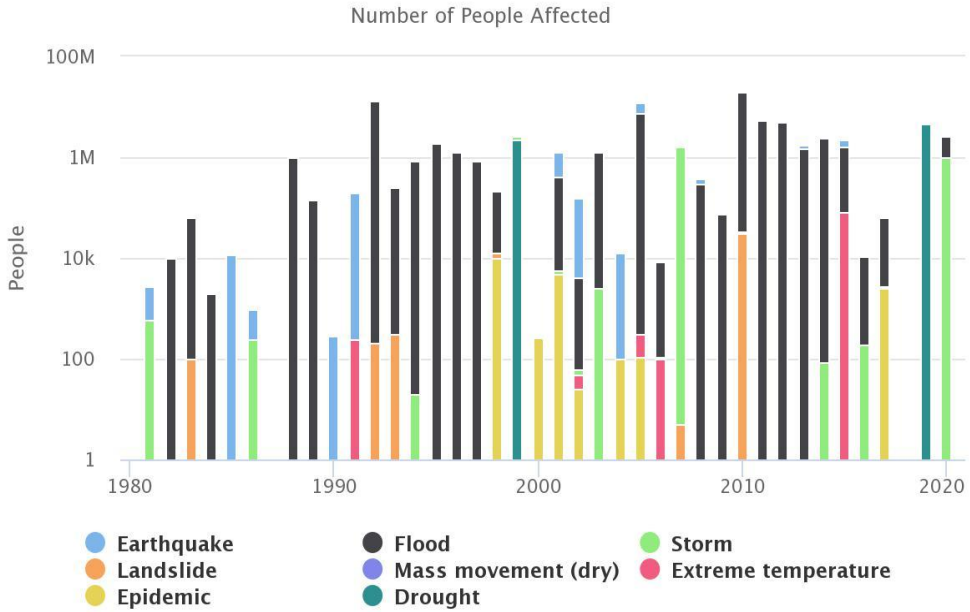

- Most severe droughts: 1952, 1969, 1971, 2000, 2001, 2002, 2015, 2018, and 2021-22.
- The drought of **1999-2002** is considered the worst drought in Pakistan's history: 3 million people were affected.
- In **2010**, the summer monsoon caused the most catastrophic flooding: 20 million people were affected.
- In heatwave **2015**, around 65,000 people were hospitalized due to heat stroke.
- Monsoon **2022** produced record-breaking rainfall: ~33 million people were affected.
- In **2023-24**, Pakistan experienced an unprecedented and prolonged spell of fog, which severely affected Punjab, KP, and upper Sindh areas.

Climate Change Triggers Extreme Events

- Climate change is causing unprecedented extreme events in Pakistan.
- Out of seven major climate extreme events, six occurred within just a 9-month period, between Jan and Sep **2022**.
- In **2023**, Cyclone “Biparjor” and a record-breaking, extended spell of fog were observed.

JAN (2022): Murree received the highest amount of snowfall.

MAR-JUN (2022): Pakistan experienced severe heat waves.

MAY (2022): Shisper Glacier GLOF event was reported in GB/upper-KP.

MAY-JUN (2022): Emergence of Flash Drought was observed.

JUN (2022): Torrential rainfall in pre-monsoon with unpre. snowfall.

JUL-SEP (2022): Deadliest floods with unpre. rainfall extremes.

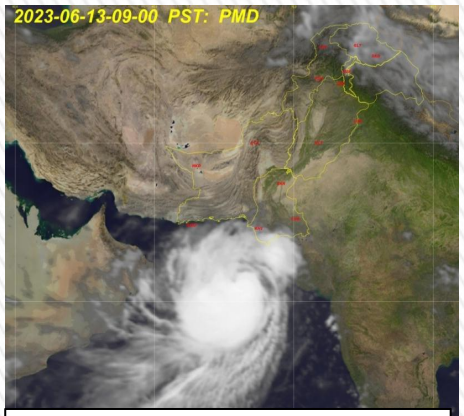

Jun (2023): Ext. svr. cyclonic storm “Biparjoy” over the Arabian Sea.

Dec-Feb (2023-24): Unprecedented and prolonged spell of fog.

Normal Rainfall Distribution in Pakistan

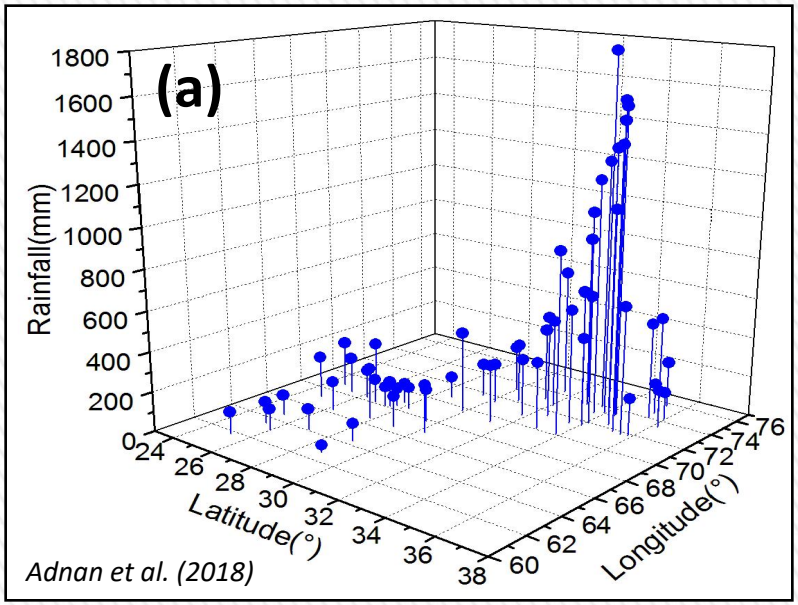

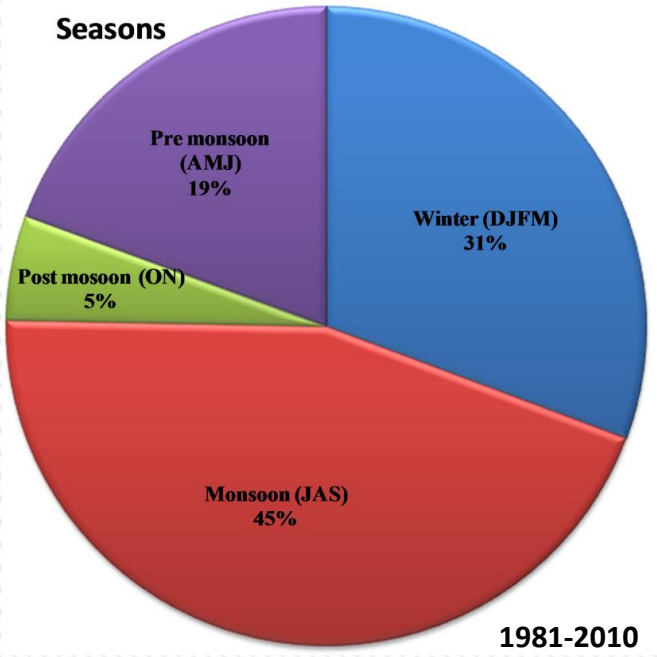

Seasonal Rainfall Distribution

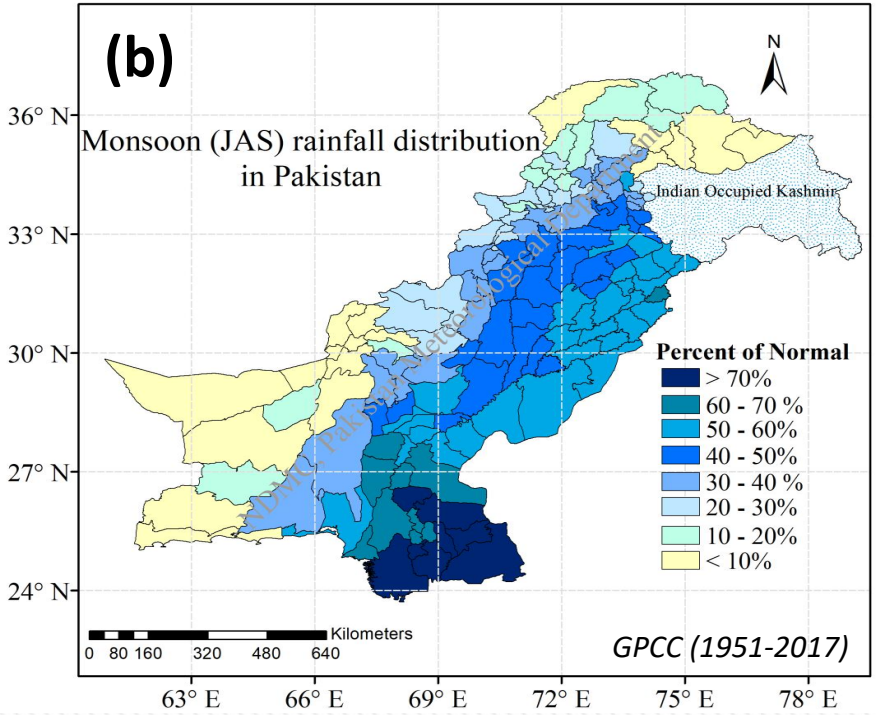

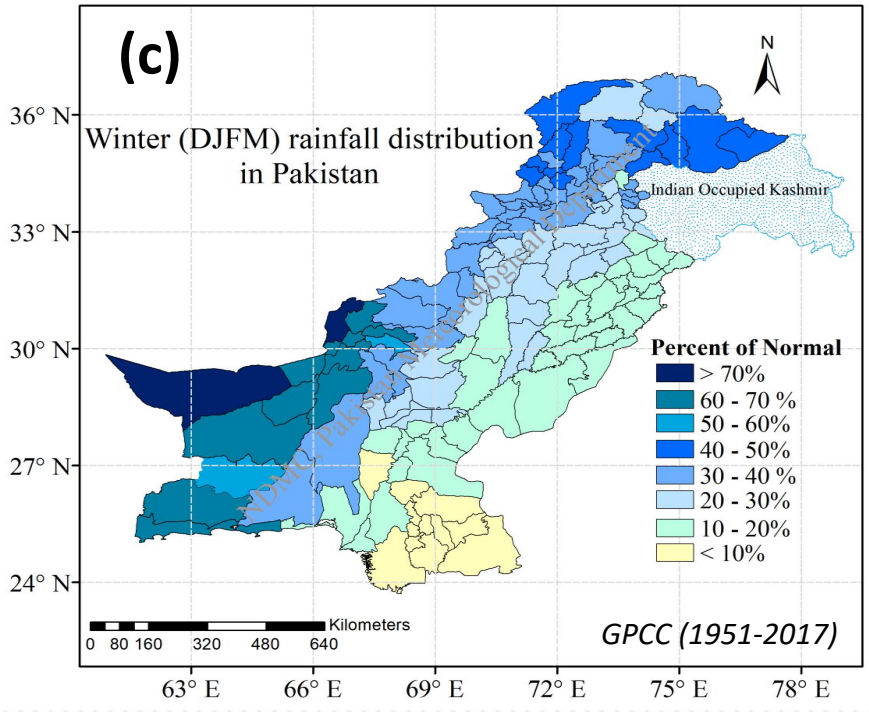

Historical Drought Patterns

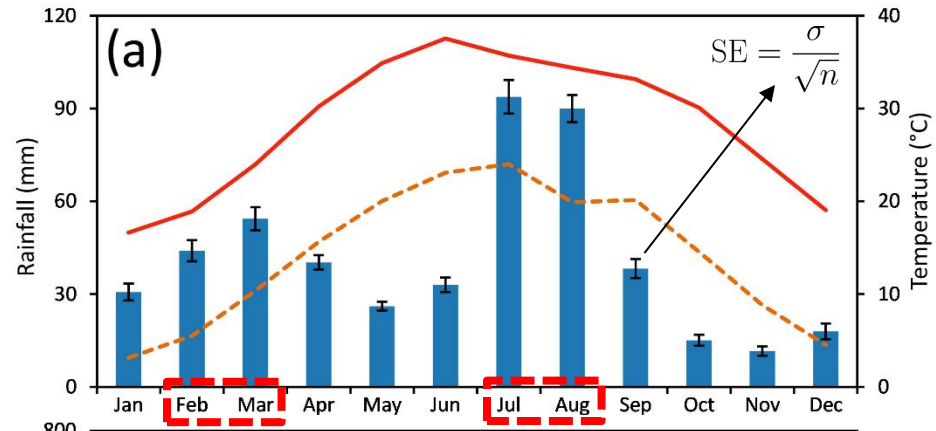

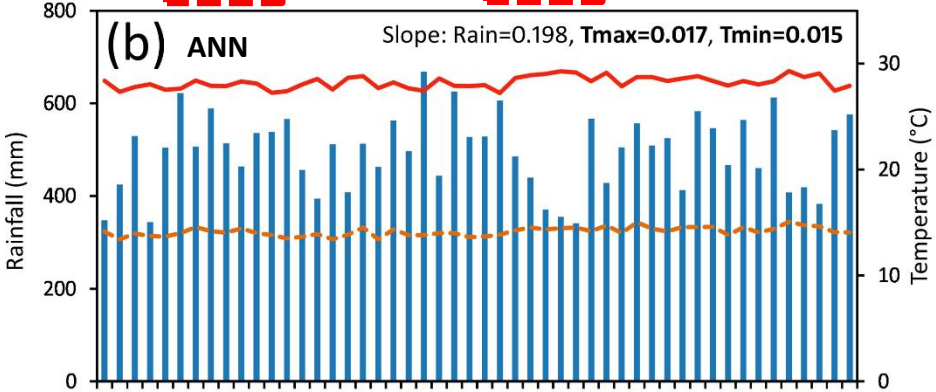

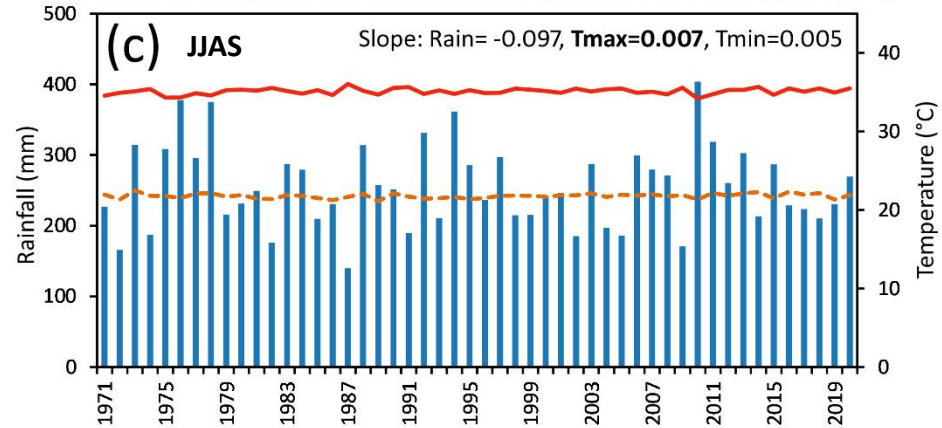

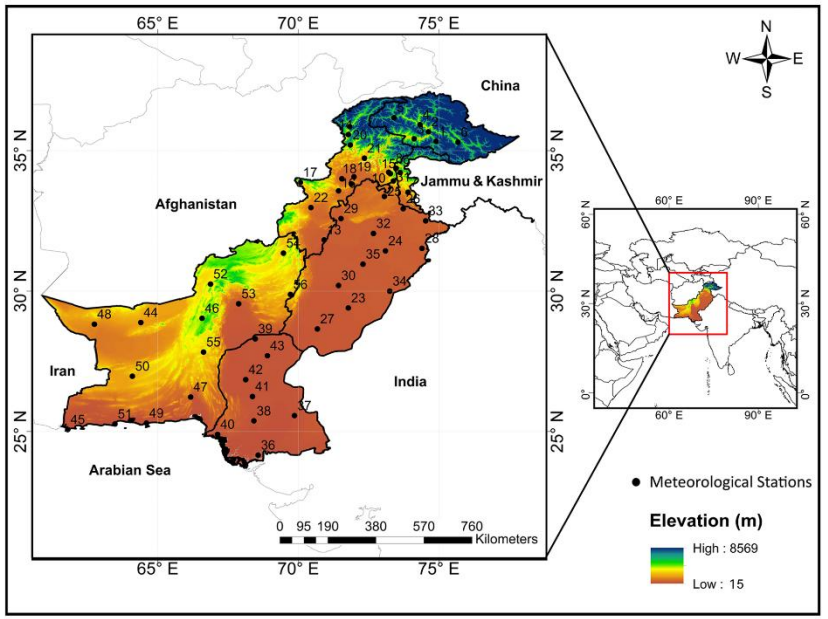

Study Area

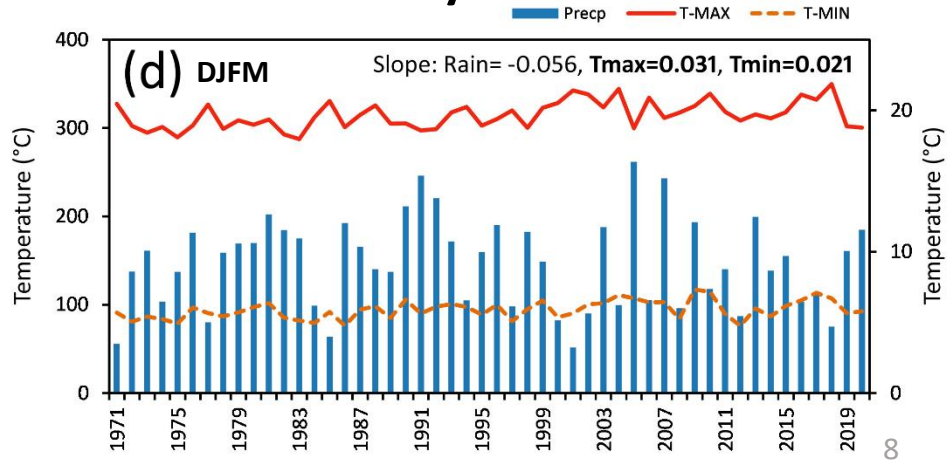

(a): Annual cycle of rainfall (bars), maximum temperature, and minimum temperature (lines) for the period 1971-2020. **(b - d):** Inter-annual variability of rainfall, maximum, and minimum temperatures on annual and seasonal timescales, respectively.

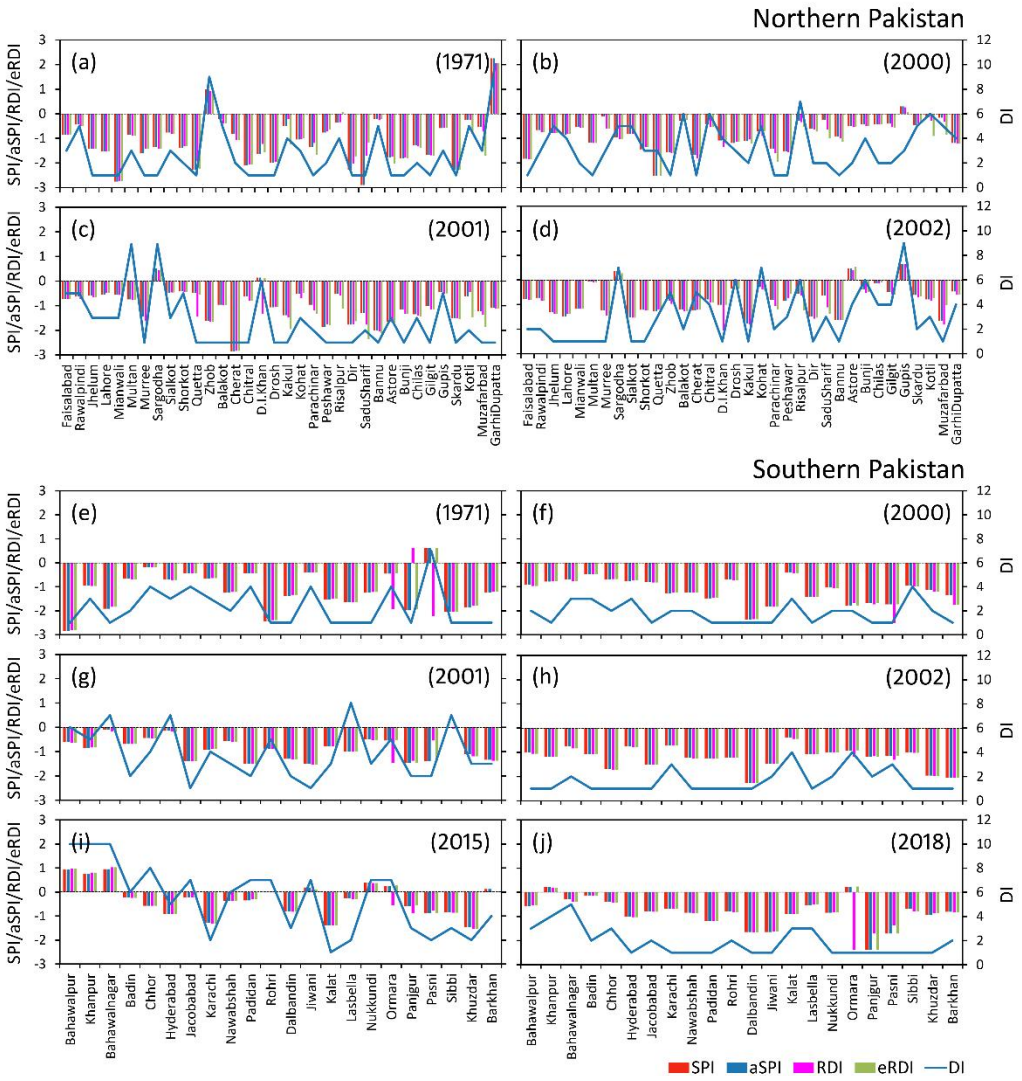

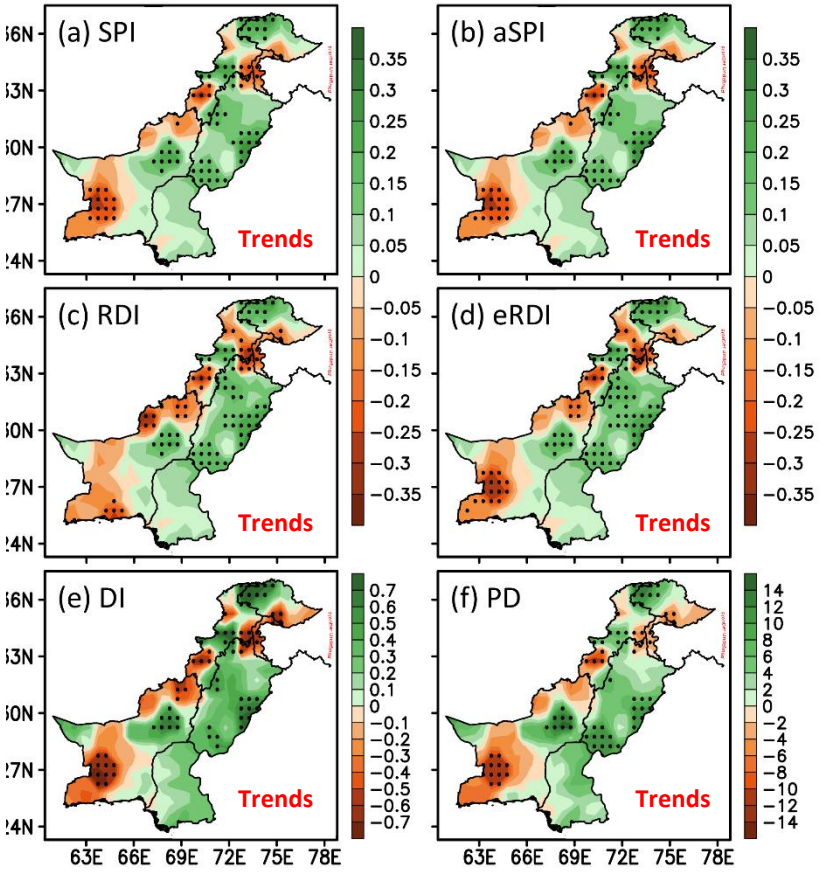

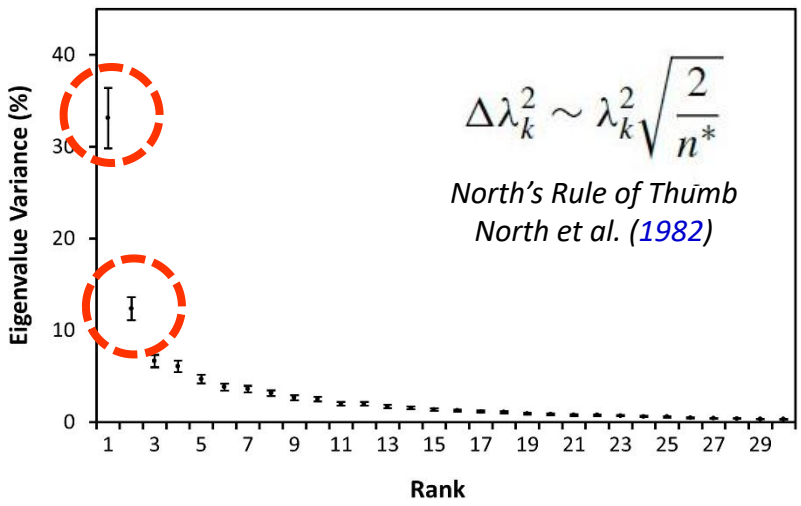

Variability of six drought indices (SPI, aSPI, RDI, eRDI, DI, PD) for the years 1971, 2000, 2001, 2002, 2015, and 2018 across N.P and S.P.

Empirical Orthogonal Function (EOF) analysis: Annual SPI

Hannachi et al. (2007 & 2021)

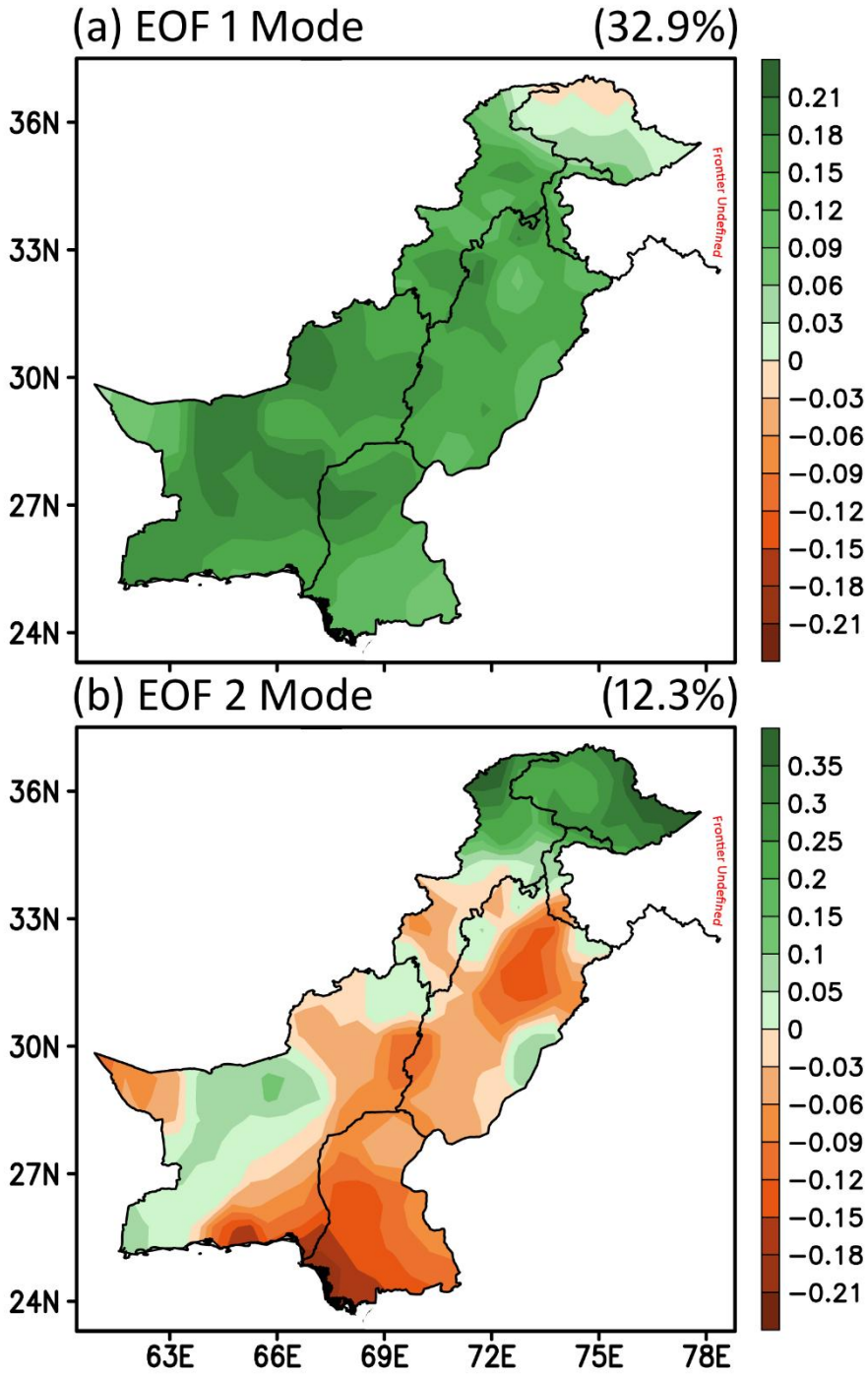
(a) EOF 1 Mode
(32.9%)
36N
33N
30N
27N
24N
0.21
0.18
0.15
0.12
0.09
0.06
0.03
0
−0.03
−0.06
−0.09
−0.12
−0.15
−0.18
−0.21
(b) EOF 2 Mode
(12.3%)
0.35
0.3
0.25
0.2
0.15
0.1
0.05
0
63E
66E
69E
72E
75E
78E

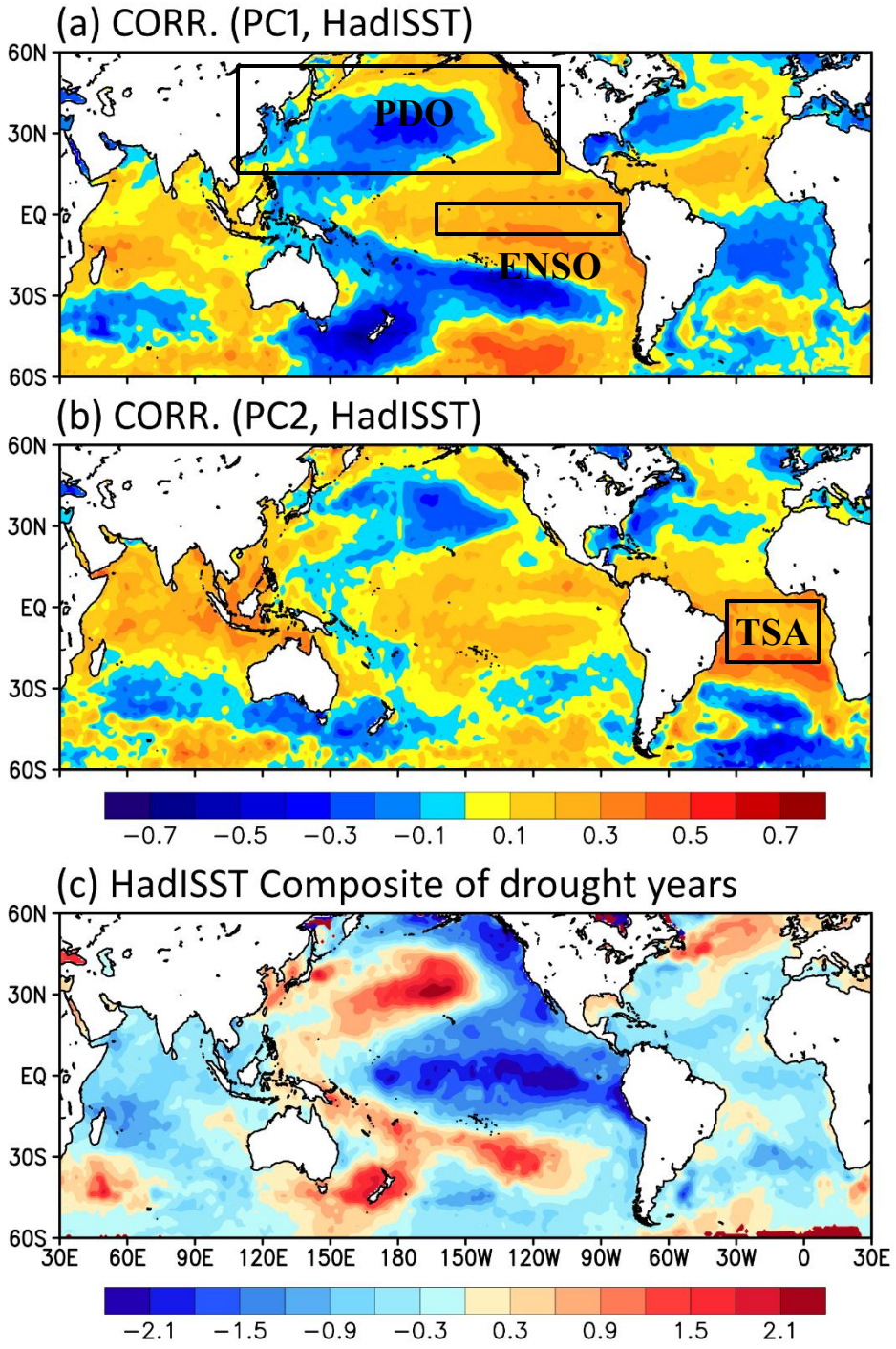
(a) CORR. (PC1, HadISST)
PDO
ENSO
(b) CORR. (PC2, HadISST)
TSA
60N
30N
EQ
30S
60S
−0.7
−0.5
−0.3
−0.1
0.1
0.3
0.5
0.7
(c) HadISST Composite of drought years
30E
60E
90E
120E
150E
180
150W
120W
90W
60W
30W
0
30E
−2.1
−1.5
−0.9
−0.3
0.3
0.9
1.5
2.1

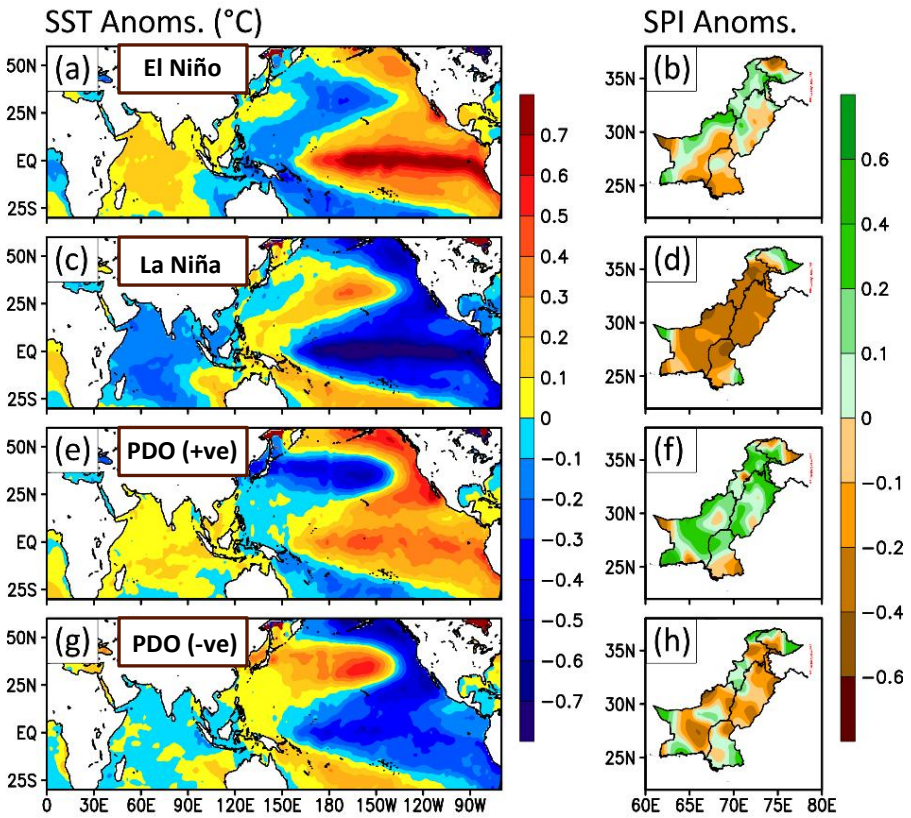

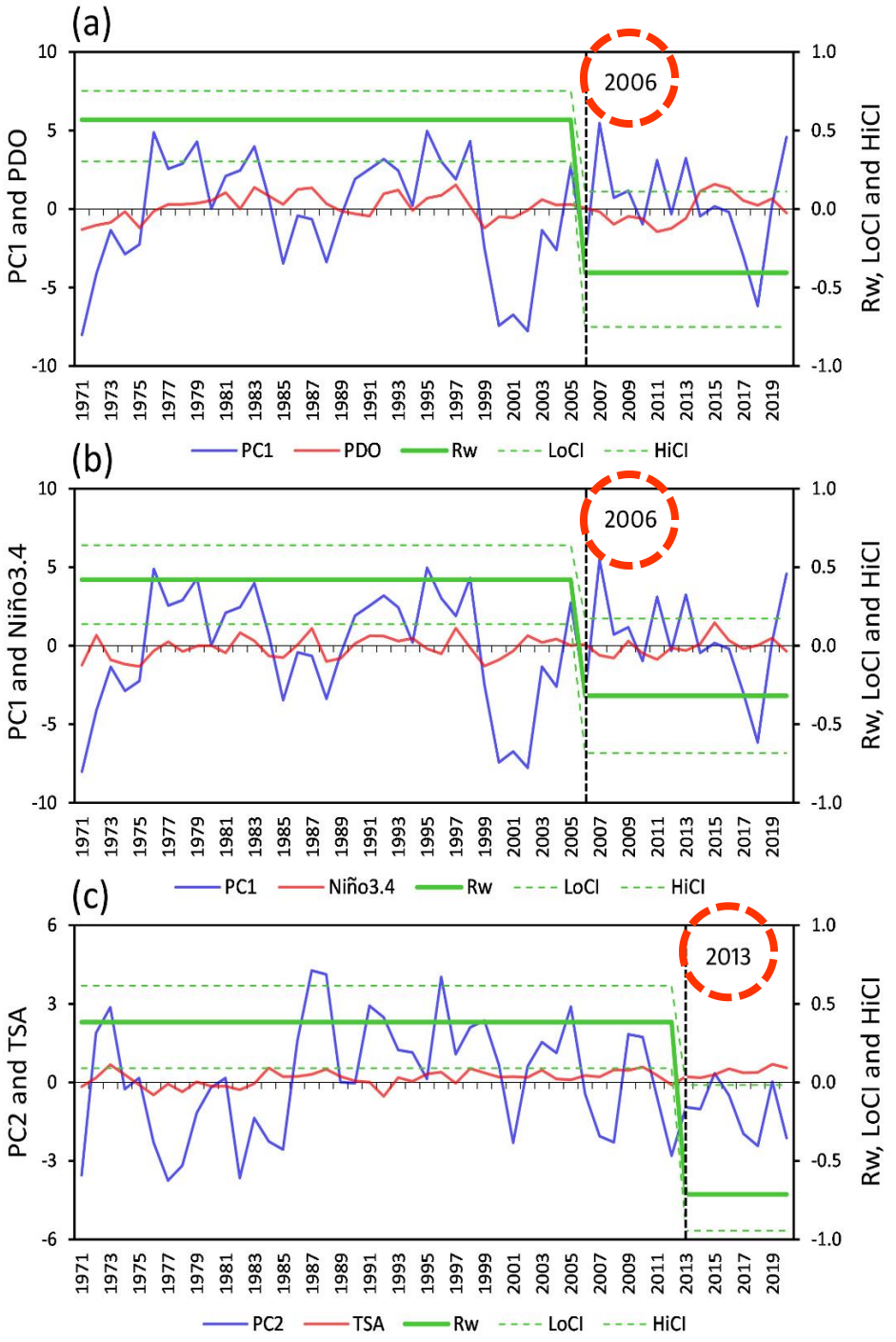

- **(a and b):** El Niño composite of SST anomalies and SPI, respectively, on annual timescale.
- **(c – d, e – f, and g – h):** Same as the first row, but for La Niña, Warm PDO, and Cold PDO composites, respectively.

Figure (right):

Regime Shift Detection

(Rodionov, 2006)

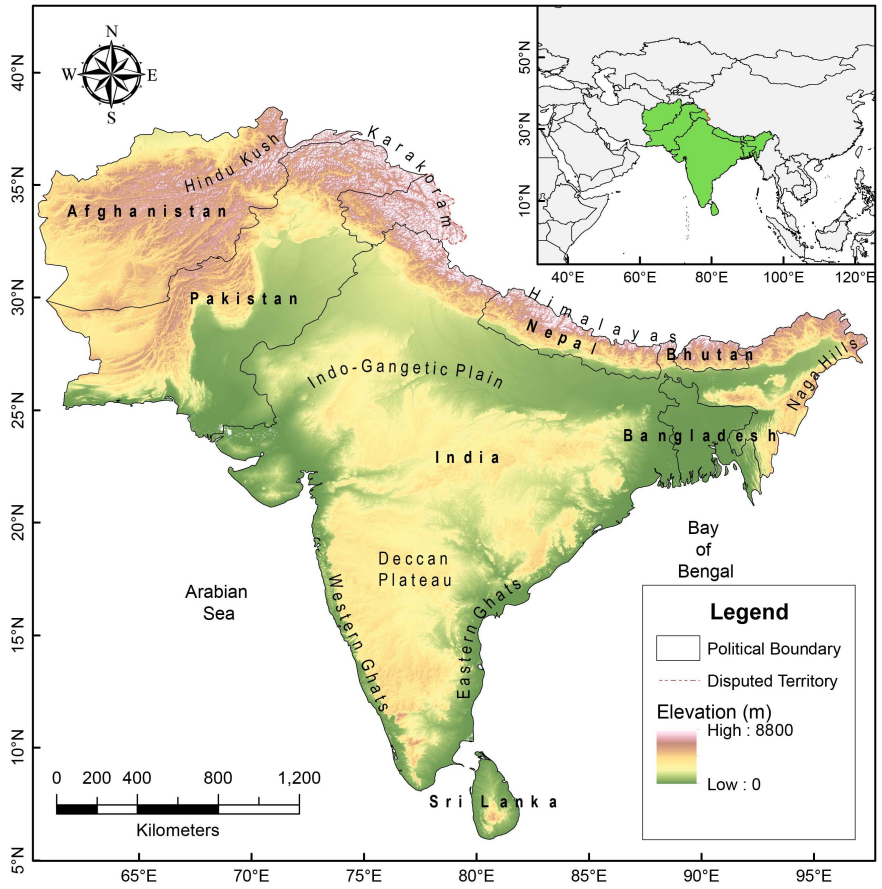

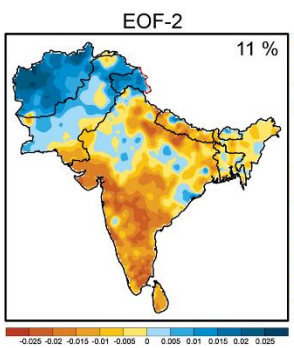

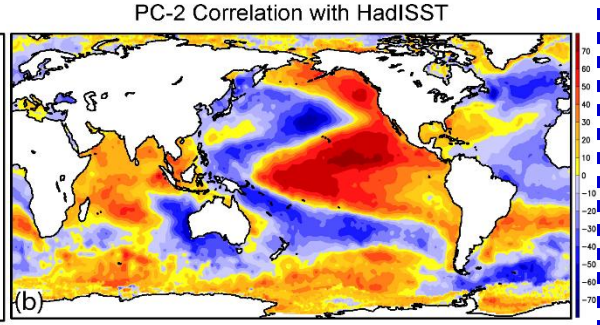

$$SPI = \frac{x_i - \bar{x}}{\sigma}$$

x_i: Annual precipitation for year i

$\bar{x}$: Mean annual precipitation

σ: Standard deviation of precipitation

Regime Shift Detection (South Asia)

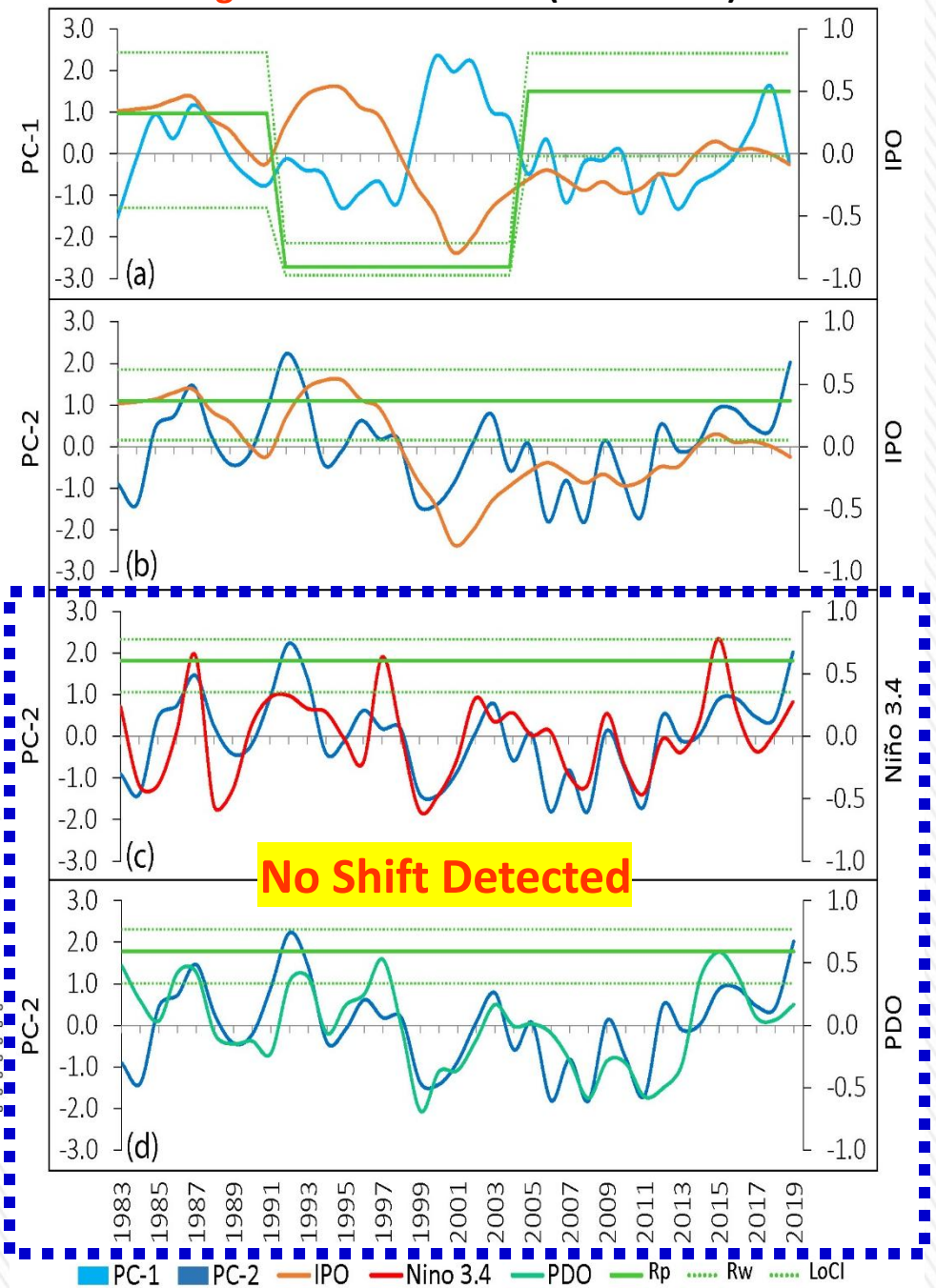

Pearson's Correlation Coefficient

$$R = \frac{\sum_{i=1}^{n}(Obs_i - \overline{Obs})\ (Sat_i - \overline{Sat})}{\sqrt{\sum_{i=1}^{n}(Obs_i - \overline{Obs})}\sqrt{\sum_{i=1}^{n}(Sat_i - \overline{Sat})}}$$

Root Mean Square Error

$$RMSE = \sqrt{\frac{\sum_{i=1}^{n}(Sat_i - Obs_i)^2}{n}}$$

Mean Absolute Error

$$MAE = \frac{1}{n}\sum_{i=1}^{n}(Sat_i - Obs_i)$$

Relative Bias

$$RB\ (\%) = \frac{\sum_{i=1}^{n}(Sat_i - Obs_i)}{\sum_{i=1}^{n} Obs_i} * 100$$

Nash Sutcliffe Efficiency

$$NSE = 1 - \frac{\sum_{i=1}^{n}(Obs_i - \overline{Obs})^2 - \sum_{i=1}^{n}(Sat_i - Obs_i)^2}{\sum_{i=1}^{n}(Obs_i - \overline{Obs})^2}$$

Probability of Detection

$$POD = \frac{H}{H + M}$$

False Alarm Ratio

$$FAR = \frac{F}{H + F}$$

Critical Success Index

$$CSI = \frac{H}{H + F + M}$$

Taylor Skill Score

$$TSS = \frac{4(1+R)^2}{(\hat{\sigma}_f + \frac{1}{\hat{\sigma}_f})^2(1+R)^2}$$

TRMM performs better followed by IMERG and GPCP.

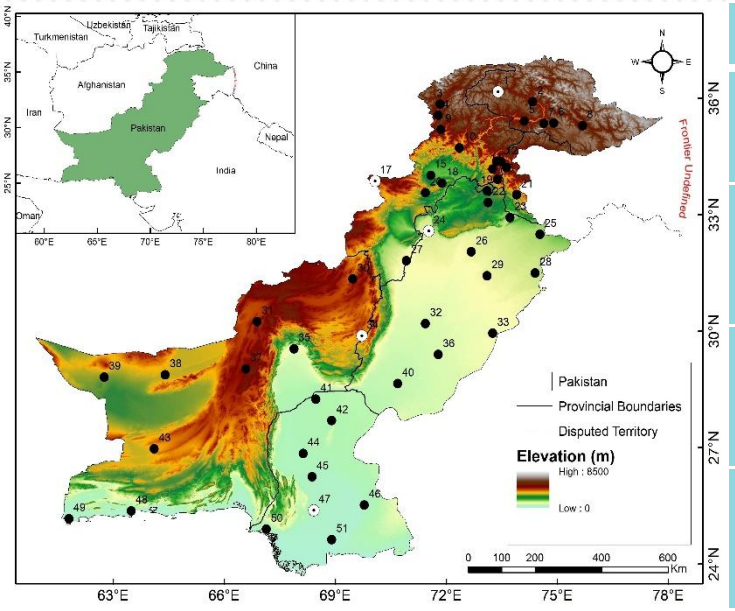

Data	Period	Res.
PMD	2000 to 2019	Point Data
TRMM	1998 to 2019	0.25° H
IMERG	2000-present	0.1° H
GPCP	1997-present	0.5° D

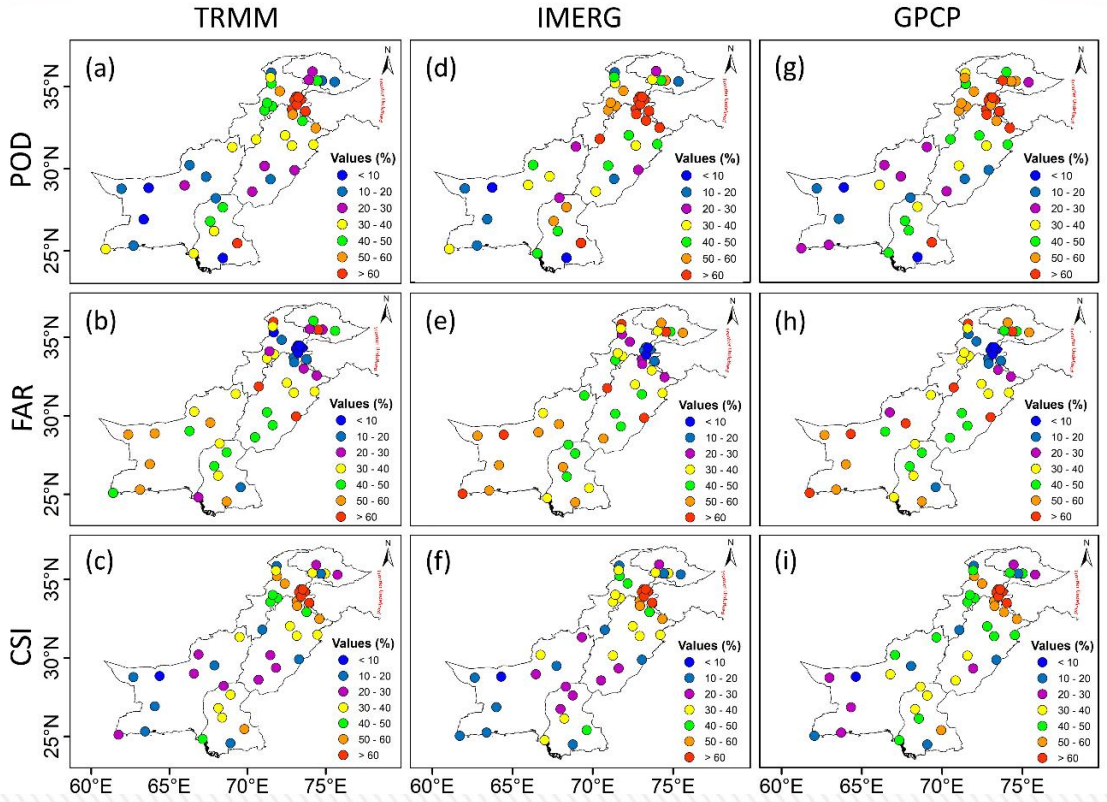

SPI-6 for the year 2002

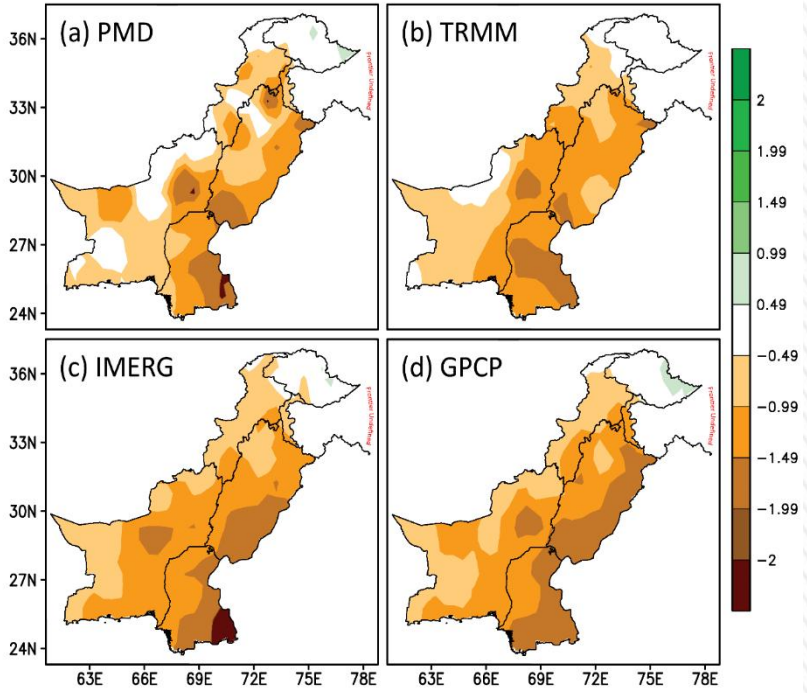

Consec. Dry Days (CDD)

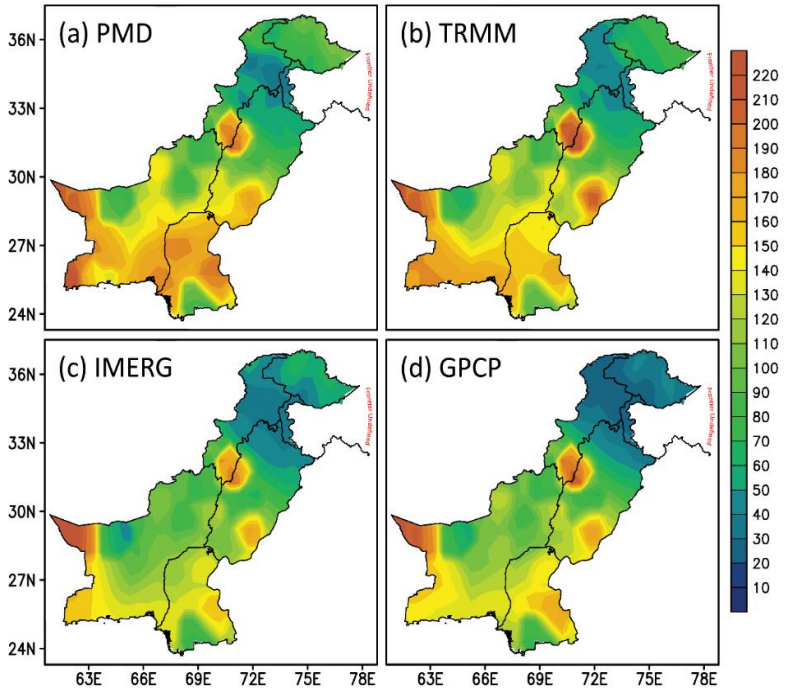

SPI-12 for the year 2002

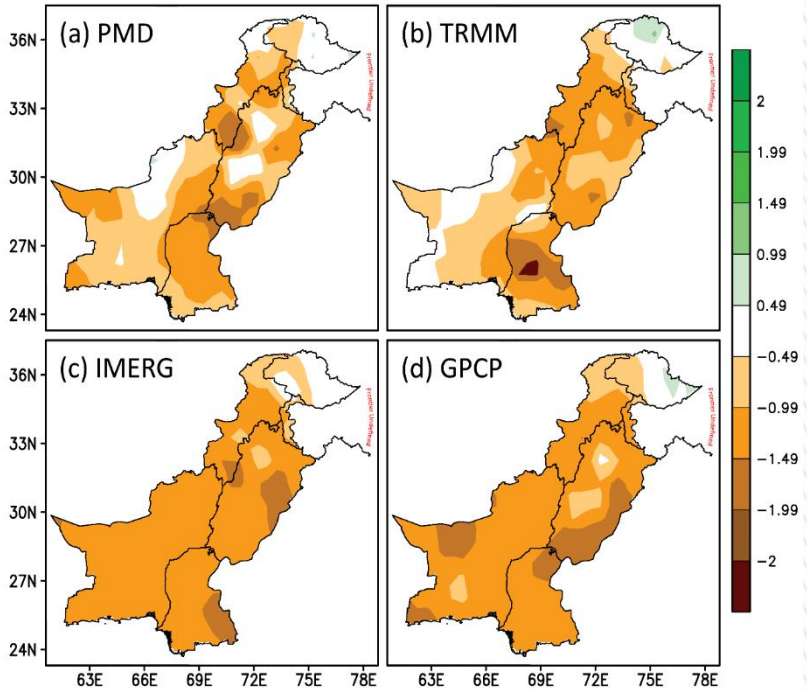

Trends (per year) CDD

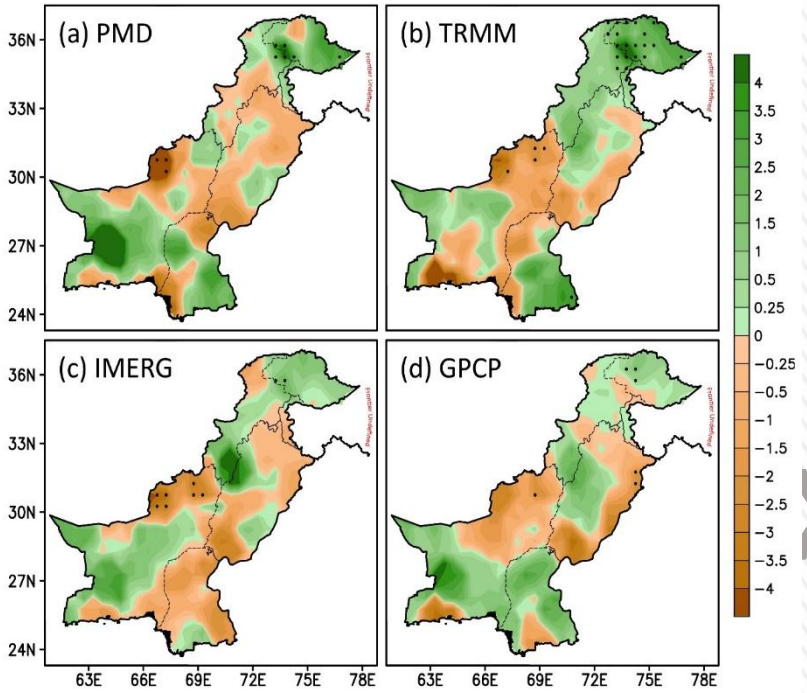

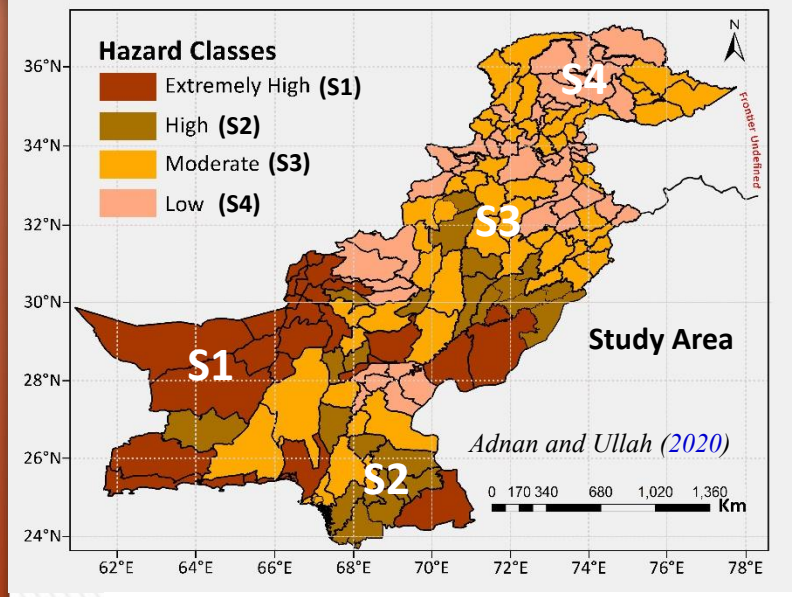

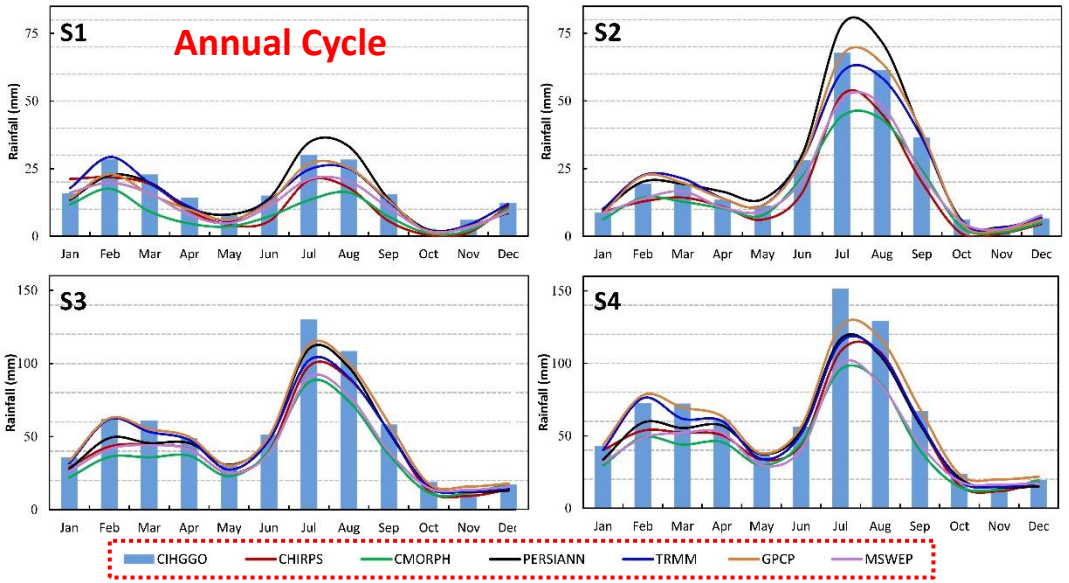

Taylor Diagram (monthly total precipitation)

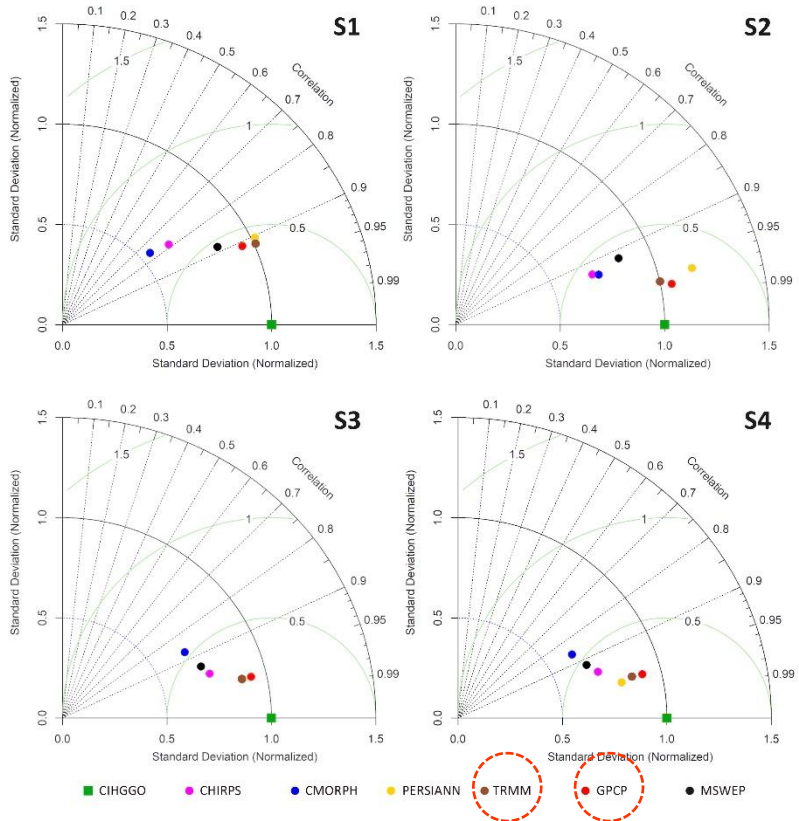

Taylor Diagram (monthly drought index: SPI-6)

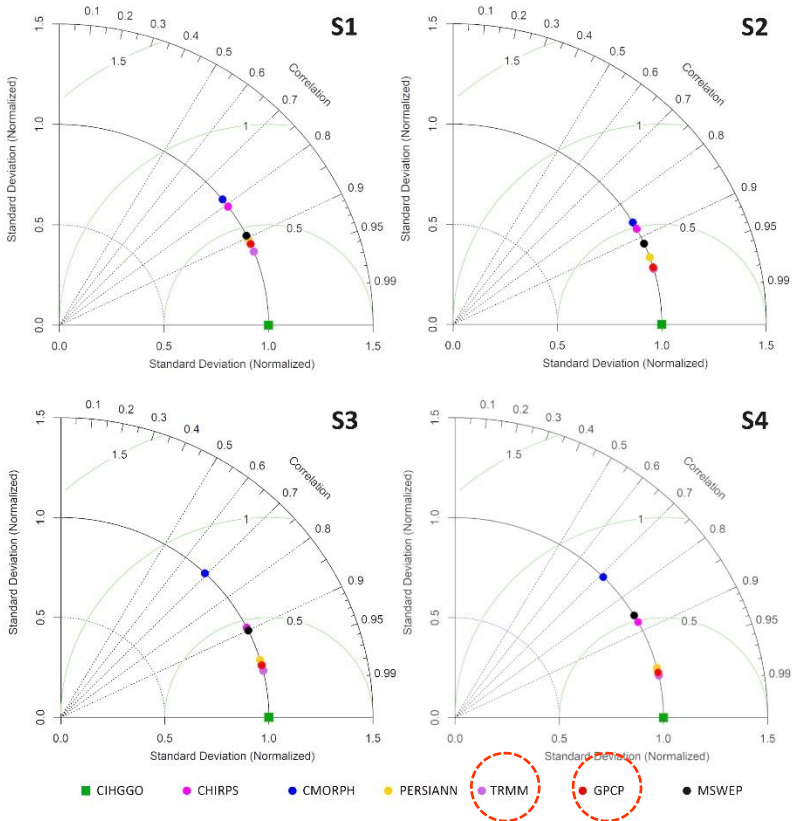

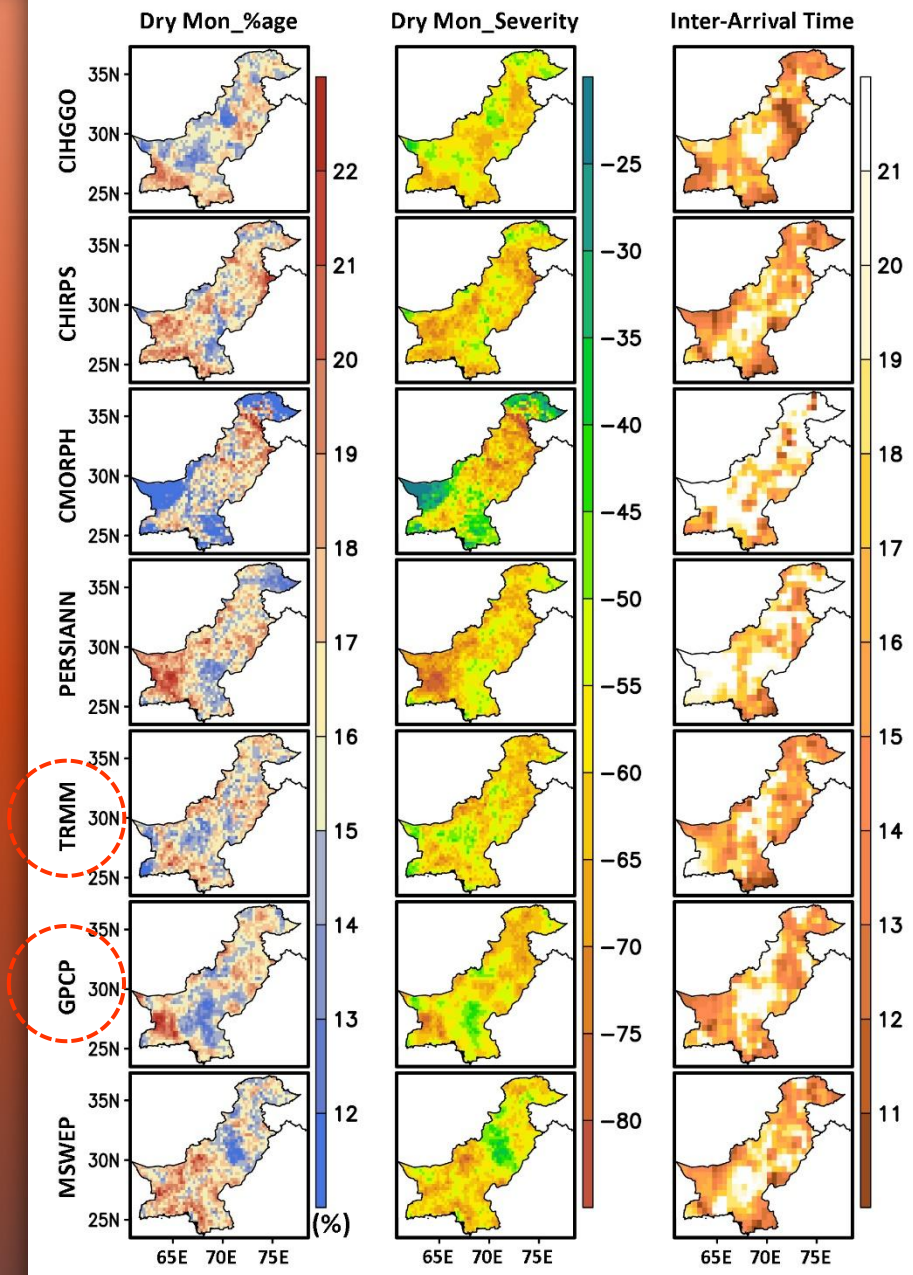

Percentage of dry months, **severity of dry months**, and **mean inter-arrival time** (in months).

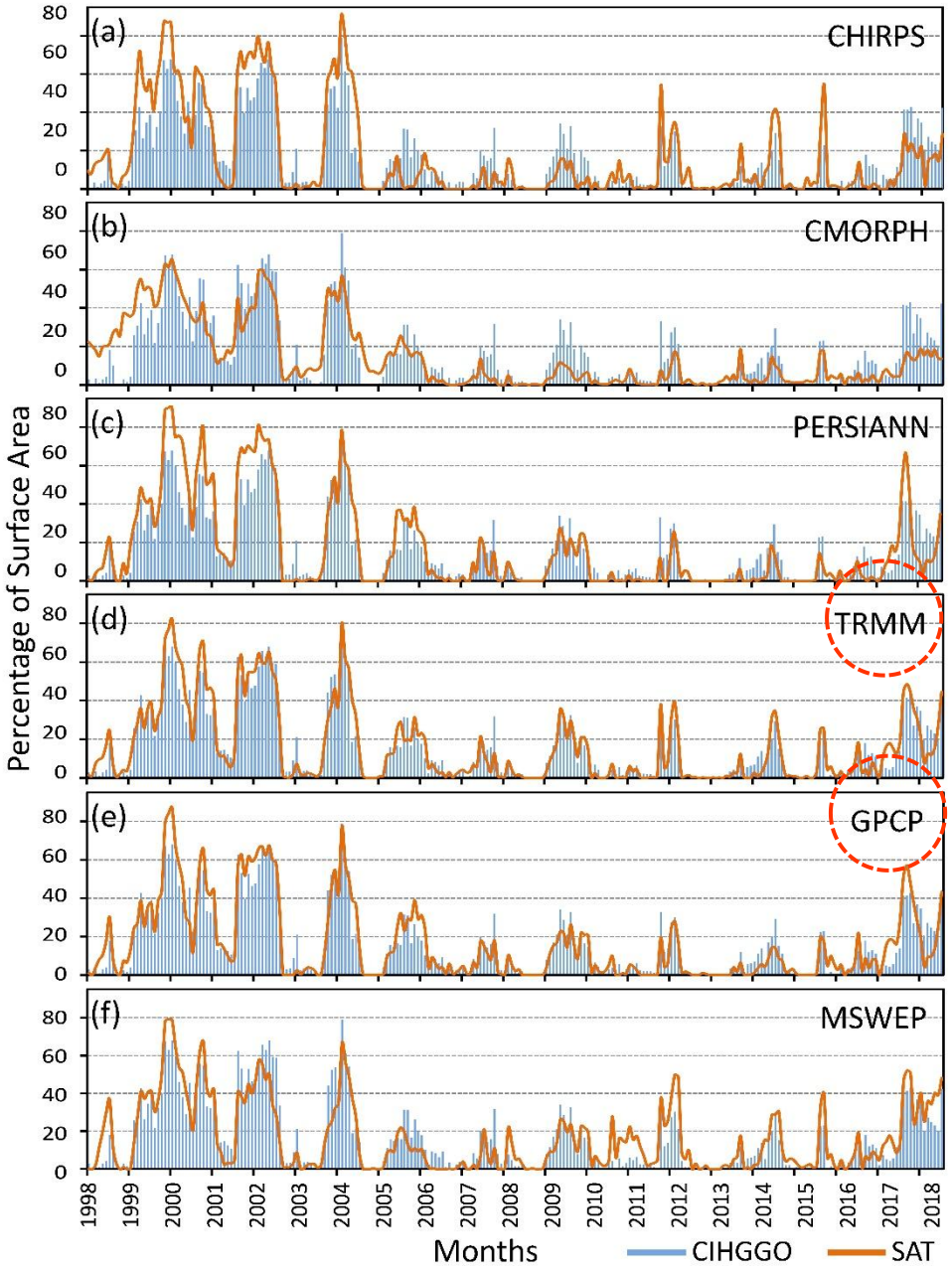

Percentage of **land area affected by drought** for each month of the study period (1998-2018).

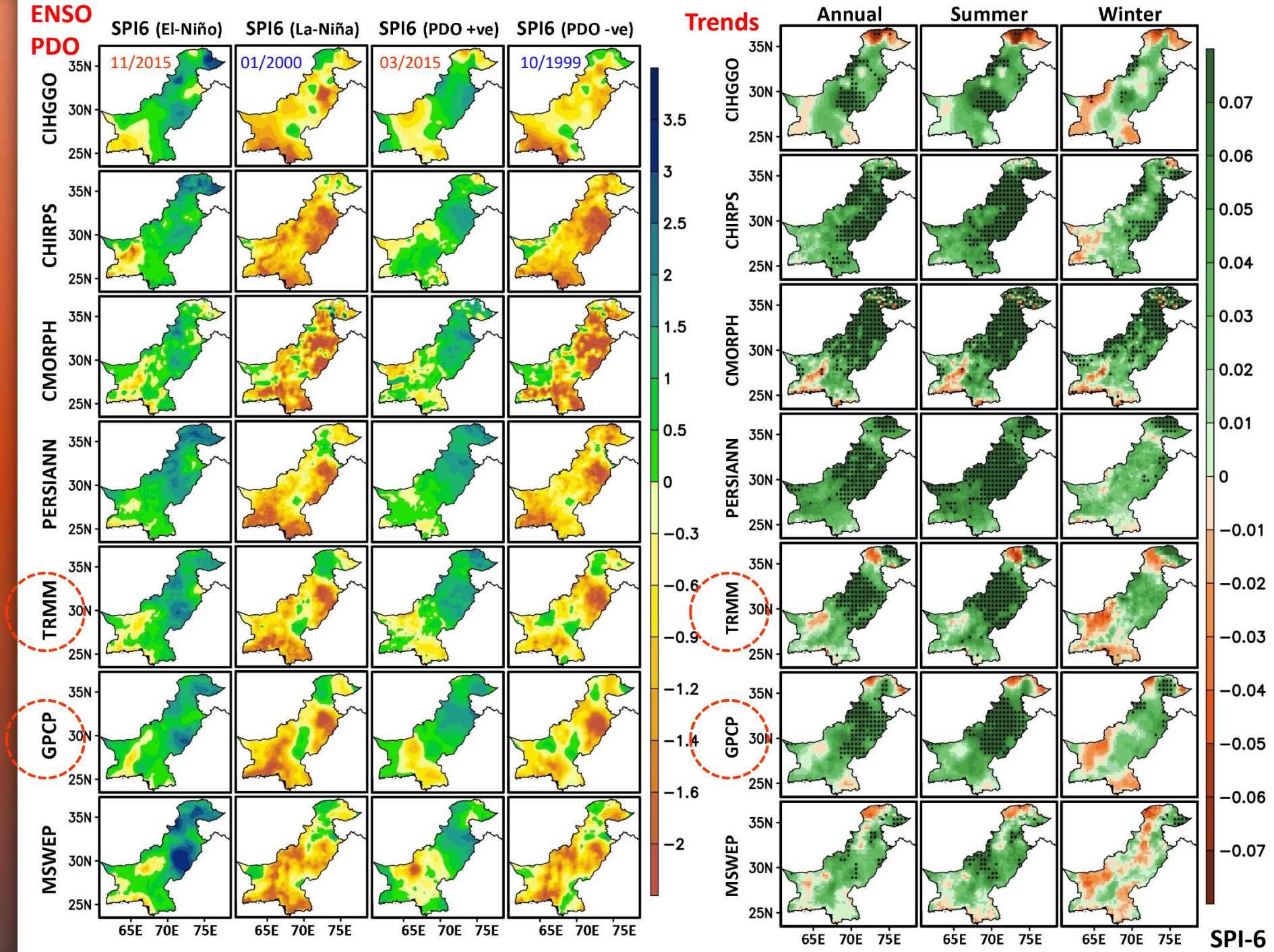
ENSO
PDO
SPI6 (El-Niño)
SPI6 (La-Niña)
SPI6 (PDO +ve)
SPI6 (PDO -ve)
11/2015
01/2000
03/2015
10/1999
CIHGGO
CHIRPS
CMORPH
PERSIANN
TRMM
GPCP
MSWEP
35N
30N
25N
65E
70E
75E
3.5
3
2.5
2
1.5
1
0.5
0
−0.3
−0.6
−0.9
−1.2
−1.4
−1.6
−2
Trends
Annual
Summer
Winter
0.07
0.06
0.05
0.04
0.03
0.02
0.01
0
−0.01
−0.02
−0.03
−0.04
−0.05
−0.06
−0.07
SPI-6

sr.	Institution	Modeling Centre	CMIP5	-CMIP6
1	CSIRO	Commonwealth Scientific and Industrial Research Organization, and Bureau of Meteorology (Australia)	ACCESS1.0 (144×192) ACCESS1.3 (144×192)	ACCESS-CM2 (144×192) ACCESS-ESM1-5 (145×192)
2	BCC	Beijing Climate Center, China Meteorological Administration, China	BCC-CSM1(160×320)	BCC-CSM2-MR (160×320)
3	CMCC	Centro Euro-Mediterraneo per I Cambiamenti Climatici, Italy	CMCC-CM (240×480)	CMCC-CM2-SR5 CMCC-ESM2
4	NOAA/GFDL	NOAA/Geophysical Fluid Dynamics Laboratory, United States	GFDL-ESM2G (90×144) GFDL-ESM2M (90×144)	GFDL-ESM4 (180×288)
5	INM	Institute for Numerical Mathematics (INM)	INM-CM4 (120×180)	INM-CM4-8 (120×180) INM-CM5-0 (120×180)
6	IPSL	L'Institut Pierre-Simon Laplace, France	IPSL-CM5A-LR (96×96) IPSL-CM5A-MR (143×144)	IPSL-CM6A-LR (143×144)
7	MIROC	National Institute for Environmental Studies, The University of Tokyo, Japan	MIROC5 (128×256)	MIROC6 (128×256)
8	MPI-M	Max Planck Institute for Meteorology, Germany	MPI-ESM-LR (96×192) MPI-ESM-MR (96×192)	MPI-ESM1-2-HR (192×384) MPI-ESM1-2-LR (96×192)

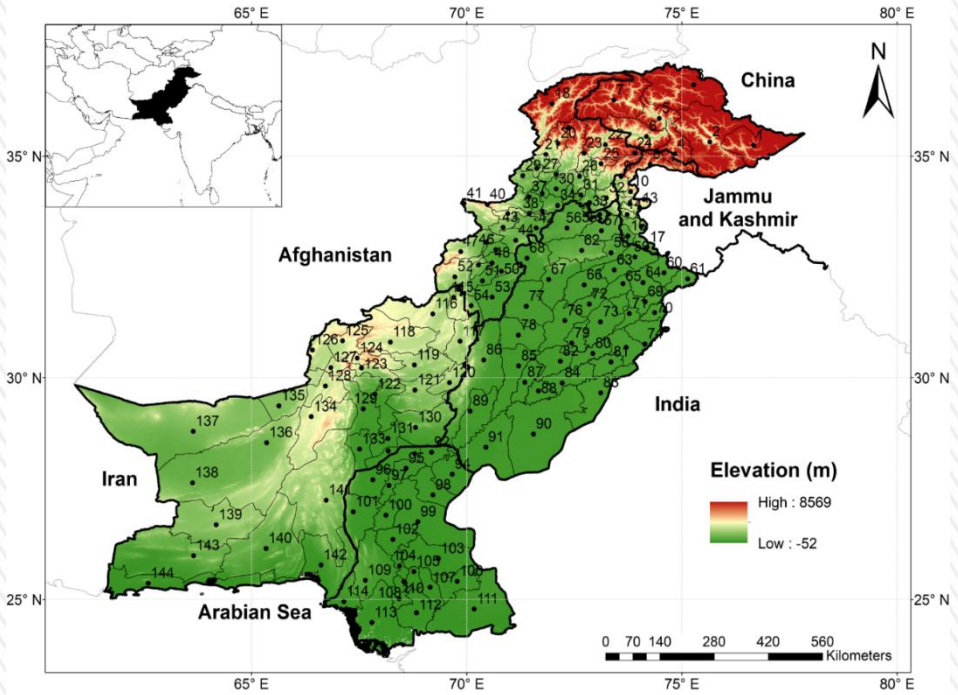

» Drought conditions are analyzed based on 36 GCM simulations (CMIP5, statistically downscaled high-resolution CMIP5, and CMIP6) using SPI and RDI indices.

» GPCC and CRU are used as reference datasets for the evaluation of climate models for historical period (1951-2005).

» 21st-century drought projections are examined based on RCP4.5 and SSP2-4.5 scenarios.

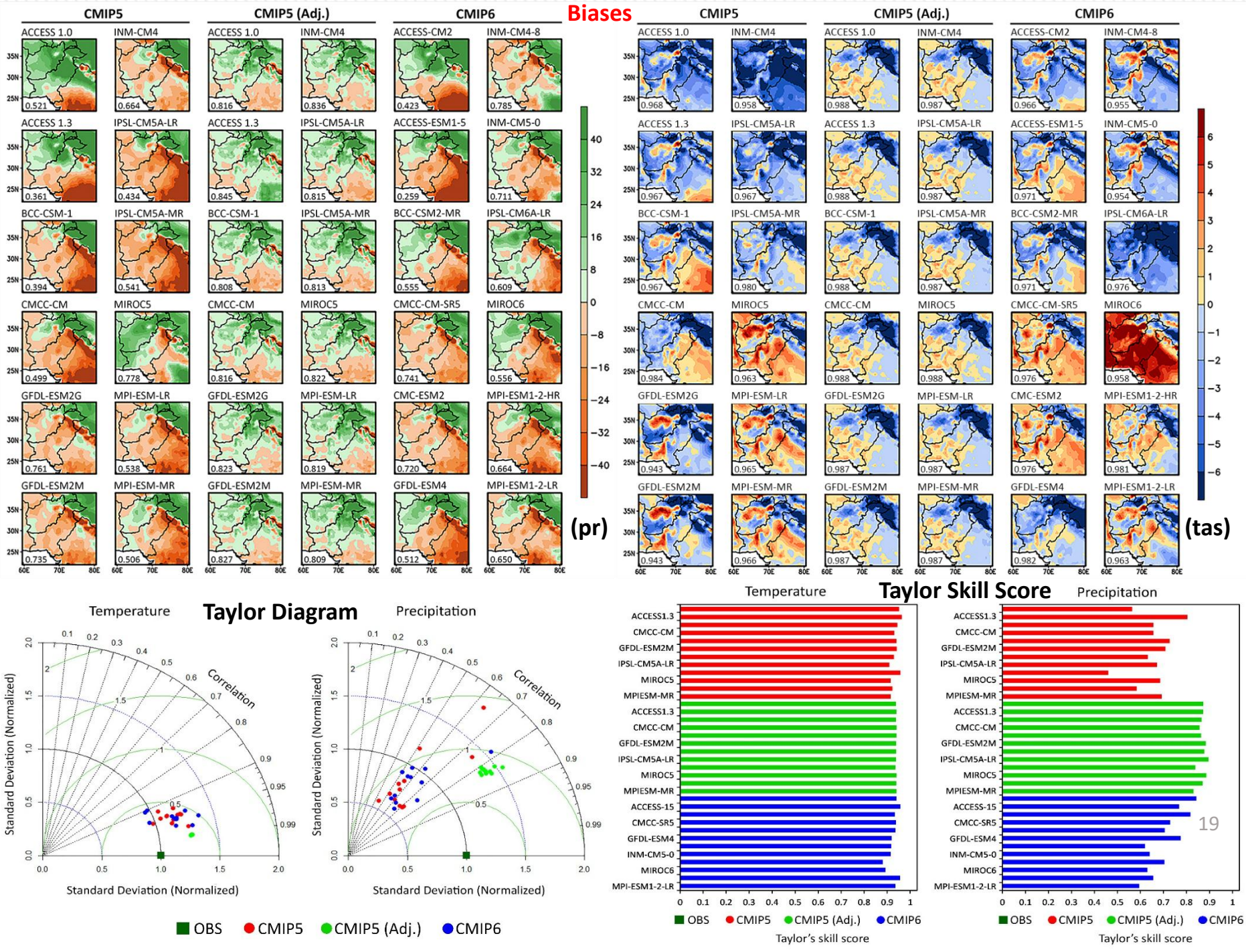
Biases
CMIP5
CMIP5 (Adj.)
CMIP6
ACCESS 1.0
INM-CM4
ACCESS-CM2
INM-CM4-8
ACCESS 1.3
IPSL-CM5A-LR
ACCESS-ESM1-5
INM-CM5-0
BCC-CSM-1
IPSL-CM5A-MR
BCC-CSM2-MR
IPSL-CM6A-LR
CMCC-CM
MIROC5
CMCC-CM-SR5
MIROC6
GFDL-ESM2G
MPI-ESM-LR
CMC-ESM2
MPI-ESM1-2-HR
GFDL-ESM2M
MPI-ESM-MR
GFDL-ESM4
MPI-ESM1-2-LR
(pr)
(tas)
Taylor Diagram
Temperature
Precipitation
Correlation
Standard Deviation (Normalized)
OBS
CMIP5
CMIP5 (Adj.)
CMIP6
Taylor Skill Score
Taylor's skill score

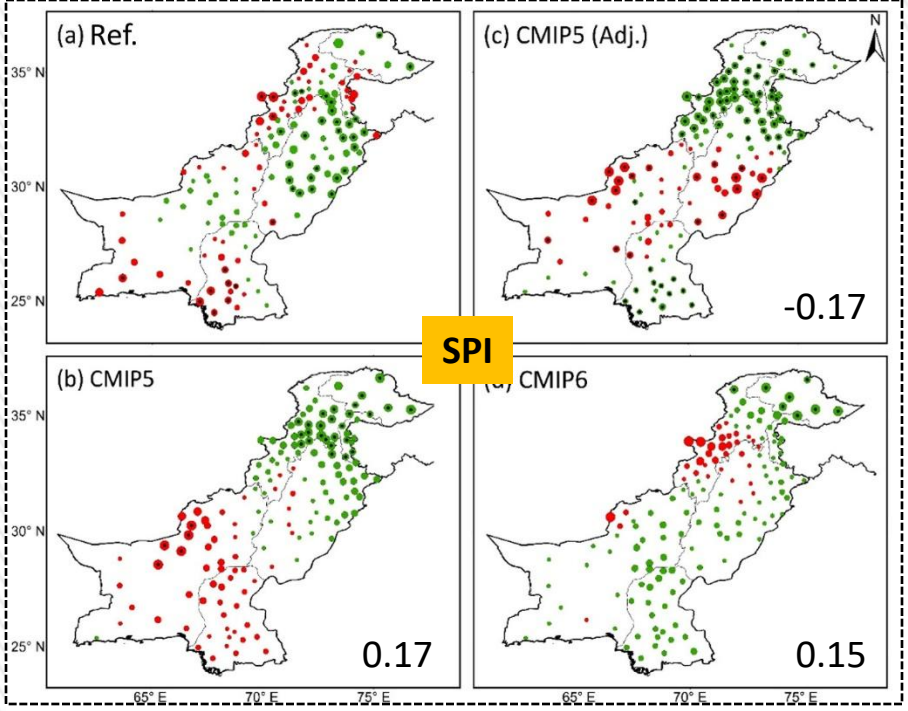

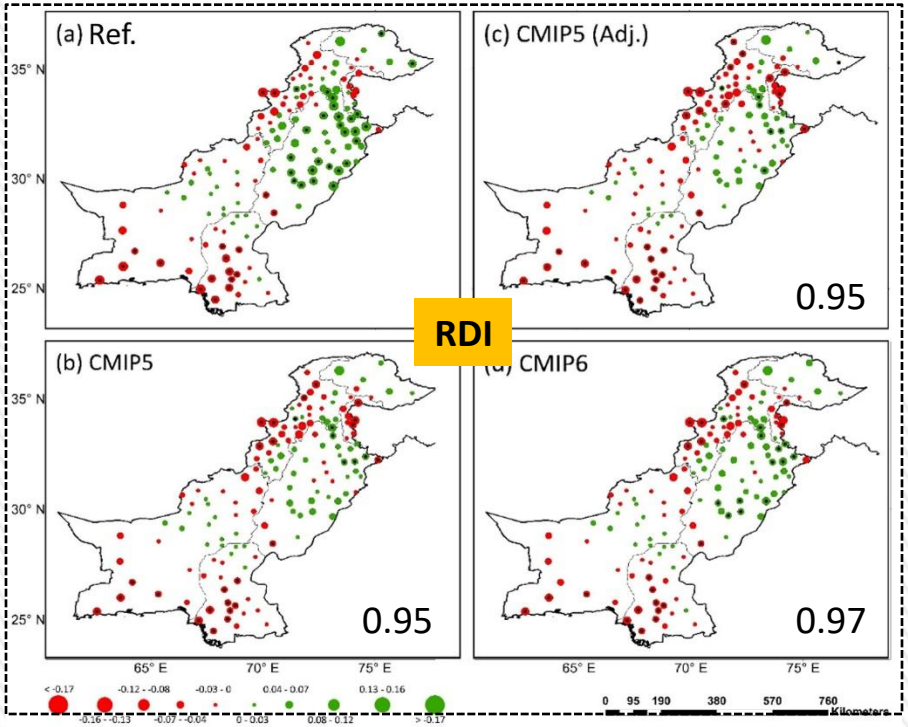

Pattern Correlation Values

SPI

Model Name	CMIP5	CMIP5 (Adj.)	CMIP6	Model Name
ACCESS1.0	-0.11	-0.18	-0.33	ACCESS-CM2
ACCESS1.3	0.10	-0.23	0.05	ACCESS15
BCC-CSM11	0.03	0.01	0.19	BCC-CSM2-MR
CMCC-CM	0.12	-0.04	0.31	CMCC-CSM2-SR5
GFDL-ESM2G	0.13	0.17	0.31	CMCC-ESM2
GFDL-ESM2M	0.40	0.07	0.02	GFDL-ESM4
INM-CM4	-0.07	-0.30	0.26	INM-CM4-8
IPSL-CM5A-LR	0.04	-0.09	-0.50	INM-CM5-0
IPSL-CM5A-MR	-0.09	-0.35	-0.02	IPSL-CM6A-LR
MIROC5	0.29	0.14	-0.14	MIROC6
MPI-ESM-LR	0.19	-0.08	0.20	MPI-ESM1-2-HR
MPI-ESM-MR	-0.17	-0.19	0.42	MPI-ESM1-2-LR
Ensemble	0.17	-0.17	0.15	Ensemble

RDI

ACCESS1.0	-0.12	-0.25	-0.49	ACCESS-CM2
ACCESS1.3	0.16	-0.23	0.06	ACCESS15
BCC-CSM11	-0.01	-0.13	0.31	BCC-CSM2-MR
CMCC-CM	0.15	0.06	0.33	CMCC-CSM2-SR5
GFDL-ESM2G	0.15	0.17	0.23	CMCC-ESM2
GFDL-ESM2M	0.43	0.16	0.03	GFDL-ESM4
INM-CM4	-0.12	-0.46	0.29	INM-CM4-8
IPSL-CM5A-LR	-0.10	-0.12	-0.50	INM-CM5-0
IPSL-CM5A-MR	-0.24	-0.48	-0.09	IPSL-CM6A-LR
MIROC5	0.35	0.17	-0.13	MIROC6
MPI-ESM-LR	0.10	-0.10	0.06	MPI-ESM1-2-HR
MPI-ESM-MR	-0.39	-0.33	0.51	MPI-ESM1-2-LR
Ensemble	0.95	0.95	0.97	Ensemble

(Upper panel): Pattern correlation between GCM's simulated slope of SPI trends (each district) and Ref. based slope of SPI trends for the period 1951 – 2005.

(Lower panel): Same as upper panel, but for RDI.

(SPI)

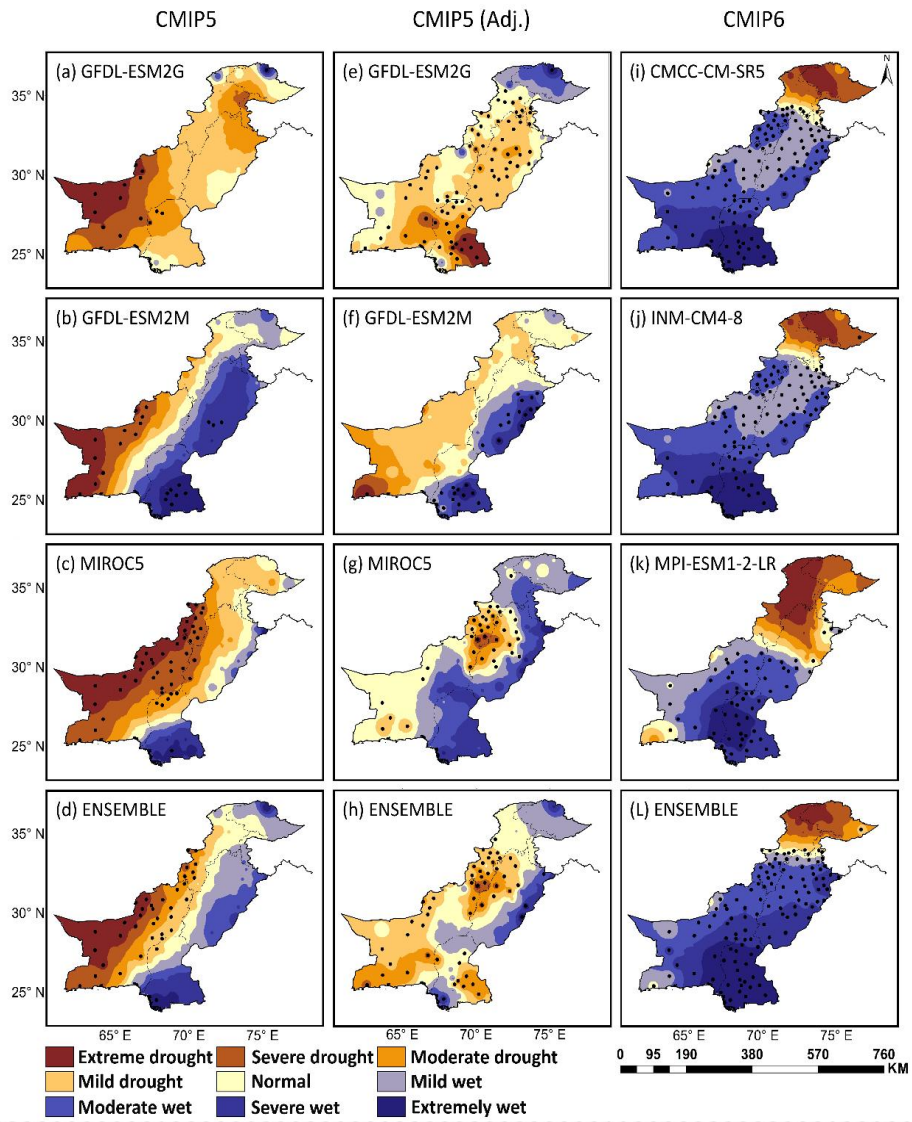

Spatial distribution of the slope of SPI for the future period: (RCP-4.5 for CMIP5 and CMIP5-Adj.) and (SSP2-4.5 for CMIP6).

(RDI)

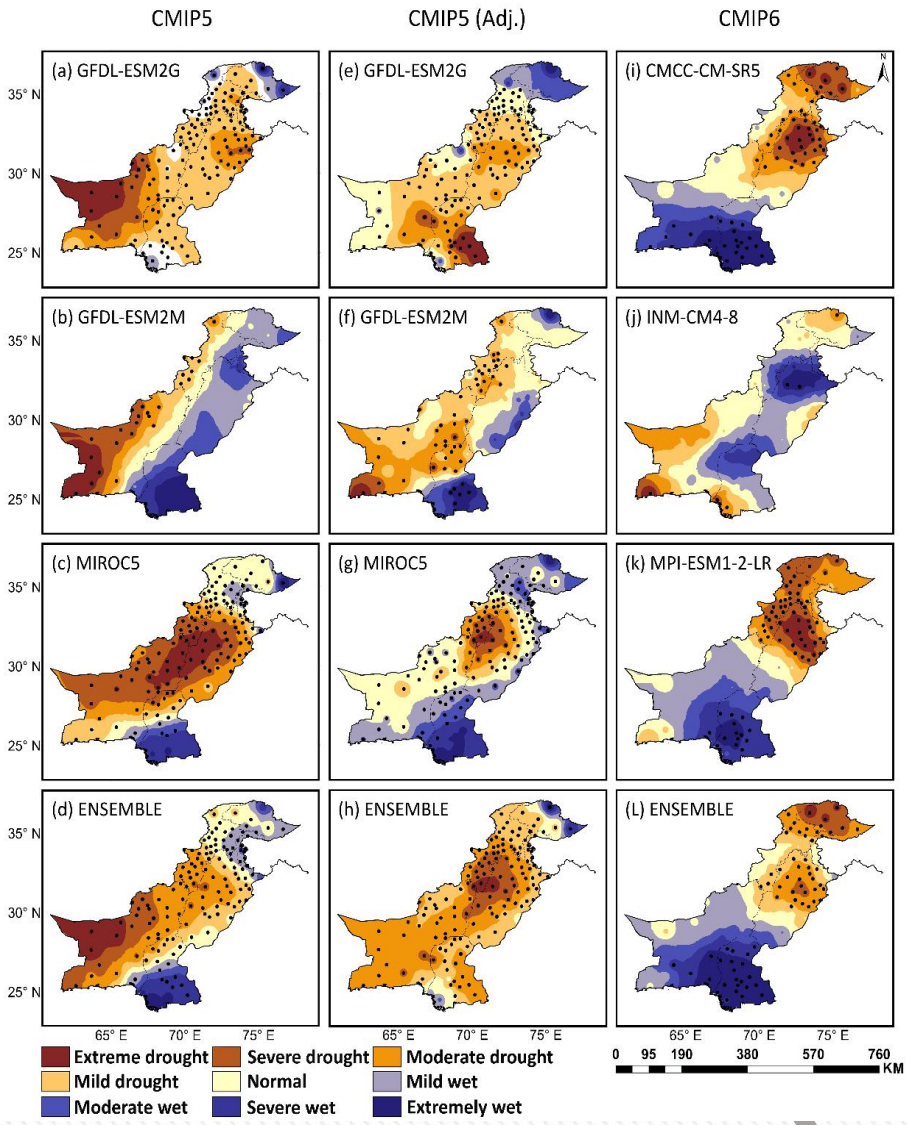

Spatial distribution of the slope of RDI for the future period: (RCP-4.5 for CMIP5 and CMIP5-Adj.) and (SSP2-4.5 for CMIP6).

Conclusions

- Climate change is actively impacting Pakistan through the increased occurrence of extreme climatic hazards.
- Prolonged and severe drought episode between 1999 and 2002 affected up to 60% of Pakistan's land area.
- Drought indices indicate wet conditions across Pakistan, except in Gilgit Baltistan, Khyber Pakhtunkhwa, and western Balochistan.
- Droughts in Pakistan are influenced by PDO, Niño3.4, and TSA indices, indicating some predictability.
- TRMM and GPCP satellite-based precipitation products perform relatively better for assessing drought in Pakistan.
- GCM data (1951-2005) show rising SPI trends (wetness) in Punjab and declining trends (dryness) in Sindh and Balochistan.
- CMIP6 models from five institutes (BCC, CMCC, INM, IPSL, and MPI-M) perform better than CMIP5.
- Future projections suggest increasing dryness in most of Pakistan's western districts.

Acknowledgment:

My sincere appreciations goes to the diligent efforts of my MS research students: **Ms. Hira Shireen**, **Ms. Sumar Munir**, **Mr. Asmad Hussain**, and **Mr. Mubahil Ahmad**, who contributed significantly to these findings. Their dedication and hard work played a crucial role in shaping the outcomes presented today.

Many thanks to **Dr. Shahzada Adnan** from the Pakistan Meteorological Department for his valuable assistance in analyzing the results, particularly his expertise in drought variability and trends.

References

- Adnan, S. and Ullah, K., 2020. Development of drought hazard index for vulnerability assessment in Pakistan. Natural Hazards, 103(3), pp.2989-3010.
- Adnan, S., Ullah, K., Shuanglin, L., Gao, S., Khan, A.H. and Mahmood, R., 2018. Comparison of various drought indices to monitor drought status in Pakistan. Climate Dynamics, 51, pp.1885-1899.
- Hannachi, A., 2021. Patterns identification and data mining in weather and climate (Vol. 10). Cham: Springer.
- Hannachi, A., Jolliffe, I.T. and Stephenson, D.B., 2007. Empirical orthogonal functions and related techniques in atmospheric science: A review. International Journal of Climatology: A Journal of the Royal Meteorological Society, 27(9), pp.1119-1152.
- Kiani, R.S., Ali, S., Ashfaq, M., Khan, F., Muhammad, S., Reboita, M.S. and Farooqi, A., 2021. Hydrological projections over the Upper Indus Basin at 1.5 C and 2.0 C temperature increase. Science of The Total Environment, 788, p.147759.
- Latif, M., Hannachi, A. and Syed, F.S., 2018. Analysis of rainfall trends over Indo-Pakistan summer monsoon and related dynamics based on CMIP5 climate model simulations. International Journal of Climatology, 38, pp.e577-e595.
- Latif, M., Syed, F.S. and Hannachi, A., 2017. Rainfall trends in the South Asian summer monsoon and its related large-scale dynamics with focus over Pakistan. Climate Dynamics, 48, pp.3565-3581.
- North, G.R., Bell, T.L., Cahalan, R.F. and Moeng, F.J., 1982. Sampling errors in the estimation of empirical orthogonal functions. Monthly weather review, 110(7), pp.699-706.
- Rodionov, S.N., 2006. Use of prewhitening in climate regime shift detection. Geophysical Research Letters, 33(12).
- Syed, F.S., Adnan, S., Zamreeq, A. and Ghulam, A., 2022. Identification of droughts over Saudi Arabia and global teleconnections. Natural Hazards, 112(3), pp.2717-2737.
- Syed, F.S., Yoo, J.H., Körnich, H. and Kucharski, F., 2010. Are intraseasonal summer rainfall events micro monsoon onsets over the western edge of the South-Asian monsoon?. Atmospheric research, 98(2-4), pp.341-346.
- Syed, F.S., Yoo, J.H., Körnich, H. and Kucharski, F., 2012. Extratropical influences on the inter-annual variability of South-Asian monsoon. Climate dynamics, 38, pp.1661-1674.

Thank You for your attention!

Additional Slides

Drought Hazard Equation

$$DHI = \frac{1}{3}\left(\frac{T_d}{T_y} + S_{Index} + \frac{SM_{i-j}}{SM_{annual}}\right)$$

T_d = total number of droughts

T_y = total number of years

S_{Index} = seasonal (winter/ monsoon) dominant rainfall index (Table); for monsoon, SM_{i-j} = soil moisture (July to December), and for winter SM_{i-j} = soil moisture (January to June); SM_{Annual} = annual soil moisture.

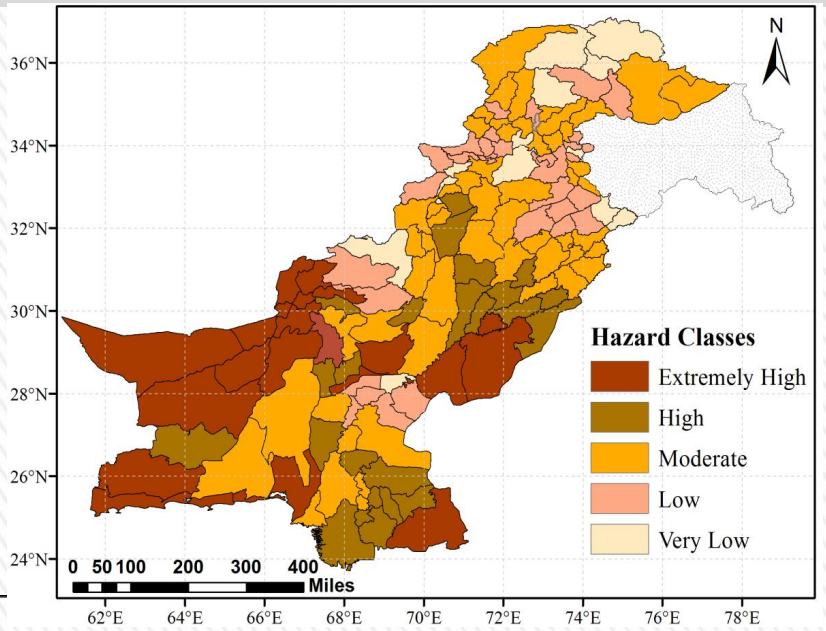

Hazard Classes	Hazard Index
Extremely High	>1.50
High	1.00- 1.50
Moderate	0.75 - 0.99
Low	0.60 - 0.74
Very Low	< 0.60

Indicator	Class limit and rating score			
Percentage of seasonal rainfall for Sindh province	> 89	79- 89	70-79	59-70
Percentage of seasonal rainfall for other province	> 60	51- 60	41-50	30-40
Index value	4	3	2	1

Classification of the Drought Severity

Sr.	Drought Severity Classes	Deciles Classification	SPI and RDI values	Percentage Departure
1	Extremely wet	10	≥ 2.0	80 to ≥100
2	Severe wet	9	1.50 to 1.99	60 to 79.9
3	Moderate wet	8	1.00 to 1.49	40 to 59.9
4	Mild wet	7	0.50 to 0.99	21 to 39.9
5	Normal	5 and 6	0.49 to -0.49	-20 to 20
6	Mild drought	4	-0.50 to -0.99	-21 to -39.9
7	Moderate drought	3	-1.00 to -1.499	-40 to -59.9
8	Severe drought	2	-1.50 to -1.99	-60 to -79.9
9	Extremely drought	1	≤ -2.00	-80 to ≤-100

1) **Percentage of dry months:** This is computed by summing the total number of dry months for the study period, then dividing by the total number of months, and subsequently multiplying by 100 to obtain the percentage value.
2) **Severity of dry months:** This characteristic is similar to the total dry months, but instead of counting the number of months, it adds the corresponding SPI value for the dry months.
3) **Mean inter-arrival time:** The interval time (in months) between two consecutive dry spells is computed for all the months in the study period. Subsequently, the time series of the inter-arrival time is calculated for each dry event. The average of the time series is the called mean inter-arrival time.
4) **Consecutive Dry Days (CDD)** is defined as three consecutive dry days with <1 mm of rainfall, CWD as three consecutive wet days with ≥1 mm of rainfall, and Total Rainy Days (TRD) as a day with ≥2.5 mm of rainfall.

La Niña from June to August

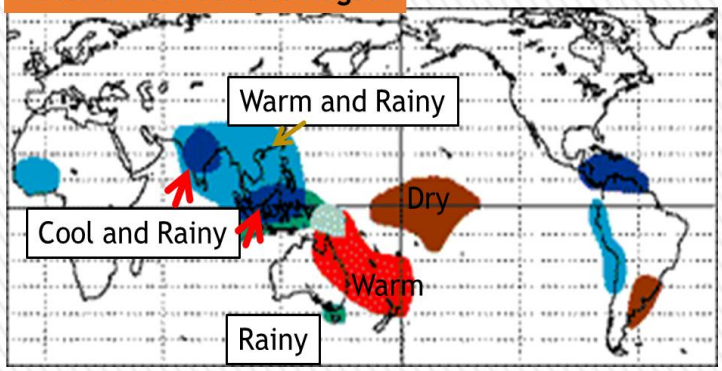

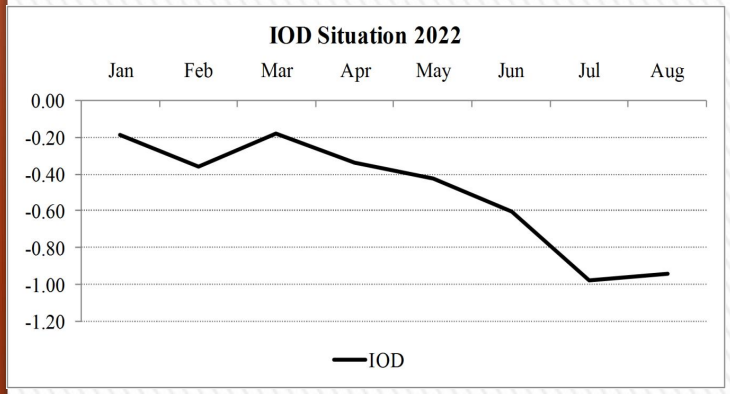

Concurrence of La Niña and negative phase of IOD during 2022 indicates anomalous warmer sea surface conditions in the eastern Indian ocean (around Indonesia), thus providing additional moisture to feed monsoon depressions during the monsoon season.

Negative Indian Ocean Dipole

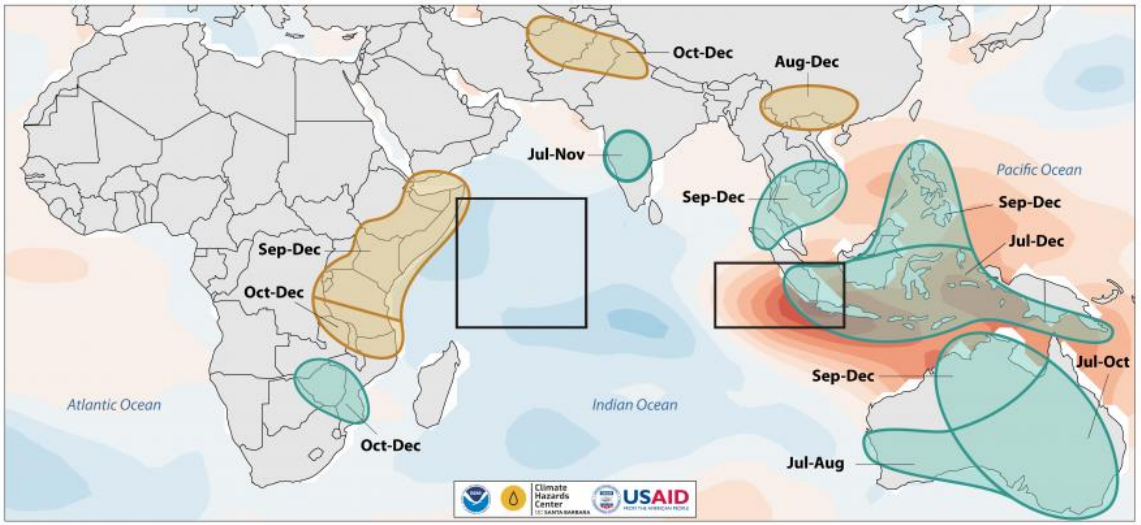

Precipitation Tendency

Wet Dry

Sea Surface Temperature Departure From Average

Below Average Above Average

Positive Indian Ocean Dipole

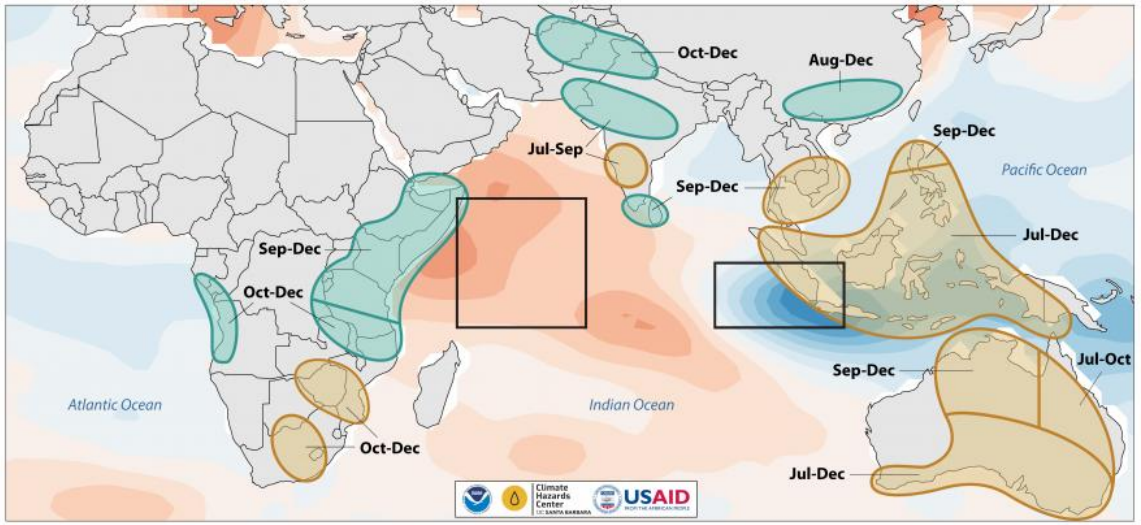

Precipitation Tendency

Wet Dry

Sea Surface Temperature Departure From Average

Below Average Above Average